

# A deep causal inference model for fully-interpretable travel behaviour analysis

Kimia Kamal<sup>\*1</sup> and Bilal Farooq<sup>†1</sup>

<sup>1</sup>Laboratory of Innovations in Transportation (LiTrans),  
Toronto Metropolitan University, Toronto, Canada

## Abstract

Transport policy assessment often involves causal questions, yet the causal inference capabilities of traditional travel behavioural models are at best limited. We present the *deep CAusal infeRence mOdel for traveL behavIour aNalysis (CAROLINA)*, a framework that explicitly models causality in travel behaviour, enhances predictive accuracy, and maintains interpretability by leveraging causal inference, deep learning, and traditional discrete choice modelling. Within this framework, we introduce a Generative Counterfactual model for forecasting human behaviour by adapting the Normalizing Flow method. Through the case studies of virtual reality-based pedestrian crossing behaviour, revealed preference travel behaviour from London, and synthetic data, we demonstrate the effectiveness of our proposed models in uncovering causal relationships, prediction accuracy, and assessing policy interventions. Our results show that intervention mechanisms that can reduce pedestrian stress levels lead to a 38.5% increase in individuals experiencing shorter waiting times. Reducing the travel distances in London results in a 47% increase in sustainable travel modes.

**Keywords:** Travel behaviour, discrete choice, structural causal learning, causal discovery, residual network, ResLogit, normalizing flow.

## 1 Introduction

Human behaviour is a complex phenomenon influenced by a variety of factors, conditions, situations, and environments. In transportation, the analysis of travel behaviour plays an essential role in supporting modellers and decision-makers to effectively plan, design, and operate transportation infrastructure and associated services. In recent years, the emergence of big data, machine/deep learning, and data science have opened new possibilities for travel behaviour analysis. The considerable ability of these models to capture underlying unobserved heterogeneity from the data has resulted in more accurate travel behaviour prediction models (Hillel et al., 2021; Kalatian & Farooq, 2021;

---

<sup>\*</sup>kimia.kamal@torontomu.ca

<sup>†</sup>bilal.farooq@torontomu.ca (corresponding author)

Wang & Ross, 2018). Despite the noticeable success in the development of advanced travel behaviour models, there are two crucial debates over the performance of these frameworks (Brathwaite & Walker, 2018; Karlaftis & Vlahogianni, 2011): 1) lack of interpretability, known as black-box nature, and 2) lack of explicit incorporation and quantification of causality—correlation does not mean causation.

In recent times, an emerging trend has been observed in the realm of travel behaviour modelling, characterized by the integration of deep learning algorithms and traditional behavioural models to leverage the respective strengths of both modelling techniques (Kalatian & Farooq, 2021; Kamal & Farooq, 2024; Sifringer et al., 2020; S. Wang et al., 2020; Wong & Farooq, 2021). These studies have mainly tried to overcome the first aforementioned restriction of deep learning algorithms in travel behavioural modelling by applying eXplainable Artificial Intelligence (XAI) methods or directly providing completely interpretable deep learning-based travel behaviour models. However, in terms of lack of causality analysis, these models can still be criticized for not isolating non-causal associations. In general, the association between a dependent variable and explanatory variables can be categorized into causal and non-causal associations. However, most travel behavioural models and deep learning algorithms ignore the effect of variables confounding the causal impact of other variables (Brathwaite & Walker, 2018). In human behaviour analysis, individual characteristics and their preference towards specific behaviour exemplify prominent instances of confounding variables. This confounding variable has the potential to influence both the policy and the desired outcome, thereby giving rise to measuring a combination of confounding and causal relationships between these variables (Pearl, 2009a).

This study primarily focuses on a noticeable contradiction and gap between the focus of advanced travel behavioural models and decision-maker’s requirements for the analysis of urban plans and policies, particularly in the context of Discrete Choice Models (DCMs). In order to bridge this gap, we aim to develop a novel framework that simultaneously employs traditional DCMs, deep learning algorithms and causal inference techniques. Briefly, our research investigates two key questions:

- What is the true causal impact of contributing factors on human behaviour?
- How would human behaviour change under an intervention in the counterfactual world?

To address these research statements, we propose the *deep CAusal infeRence mOd-eling for traveL behavIour aNalysis (CAROLINA)* framework. *CAROLINA* framework first tries to guarantee both the interpretability and causality by integrating the ResLogit and Ordinal-ResLogit structures with the causal inference techniques. These ResNet-based model structures are deep interpretable learning discrete choice frameworks used for both ordinal and categorical datasets (Kamal & Farooq, 2024; Wong & Farooq, 2021) and *CAROLINA* is a logical causal-based continuation of these ResNet-based frameworks. It is worth noting that *CAROLINA* is still classified as a probabilistic behaviour model, where our focus is on causal association rather than a combination of causal and non-causal association. Secondly, in order to provide insights into the effects of manipulation on the system, we overcame the fundamental differences between causal inference and statistical analysis. Particularly, in the forecasting step, we incorporate the fact that observational and post-intervention systems are not identically

distributed. In fact, once an external intervention is imposed on the system, it induces changes in the causal structure and causal mechanisms of the model, consequently resulting in the emergence of counterfactual distributions. Furthermore, counterfactual analysis offers valuable insight at the individual level by considering how people imagine themselves in a counterfactual world, ask counterfactual-based questions, and make optimal decisions. For instance, pedestrians may unconsciously ask themselves “what would have happened if I had crossed the road immediately without attention to vehicles” or employees may think daily, “imagine if we would have gotten used to using active modes! In this study, we try to propose a novel idea for estimating counterfactual human behaviour by considering both latent variables and intervention impact based on causality analysis.

To evaluate the performance of our proposed model structures, we use three datasets with exclusive properties. First, as Virtual Reality (VR) dataset has recently received great attention in recent transportation research, particularly in the context of futuristic scenarios such as the interaction between Automated Vehicles (AVs) and other road users, we use a novel VR dataset to analyze pedestrian crossing behaviour. The VR dataset is collected by immersing the participants in artificial computer-generated experiences (Farooq et al., 2018). Secondly, we use a Revealed Preference (RP) dataset to assess the causal structure underlying travel behaviour choices. Finally, to clarify the differences between a typical behavioural modelling approach in transportation and our causal-based method, we make use of a synthetic dataset.

In short, *CAROLINA* framework aims to provide causal-based association analysis, improve predictive accuracy, and retain interpretability and our study contributes to the transportation literature in the following way:

- Formulation of an interpretable deep causal-based behavioural model.
- Formulation of a generative counterfactual model which to the best of our knowledge, this effort represents the first investigation in transportation.
- Analysis of causal impacts of intervention in transportation systems.

The rest of this paper is organized as follows. First, a brief review of the literature on causality analysis in transportation, causal discovery and structural causal model is provided. It is followed by the methodology section in which the structure of the two proposed models is described in detail. In section 4, a description of datasets is presented and then the analysis of estimated models for these data and synthetic datasets are provided in section 5. Finally, in the conclusion section, some suggestions and future directions for the study are proposed.

## 2 Background and Definitions

This section begins with a brief overview of causality analysis in transportation studies. Subsequently, we provide a concise review of Causal Discovery and the Structural Causal Model as an approach to conducting causal inference in this study.

## 2.1 Causality analysis in transportation studies

In the realm of transportation, travel behaviour modelling as a predictive tool typically relies on observational data to anticipate future conditions of the transport system. This approach assumes that both the observed and future systems share identical distributions, implying that our predictions remain valid as long as the system remains unchanged. Nevertheless, when it comes to assessing future policy impact, decision-makers and policymakers are interested in forecasting the system's behaviour in a counterfactual world, after implementing some changes. This introduces a causal dimension, where the focus shifts to answering causal-based questions (Rubin, 2019). In transportation, the self-selection problem, which is rather a common issue, has been encouraging transportation researchers to primarily focus on causality analysis (Mokhtarian & Cao, 2008). This phenomenon arises when individuals self-select into certain travel behaviour choices due to their preferences, attitudes, personal characteristics, or other unobserved variables, resulting in a biased estimation of the effect of contributing factors on travel behaviour outcomes. In the discipline of causal inference, this concept is known as confounding impact, meaning that some variables may not only influence a travel behaviour outcome, but also are correlated with policies. In fact, the estimated relationship between the variables of interest and travel behaviour outcomes may be confounded by the self-selection bias. Consequently, any differences in travel behaviour outcomes observed among individuals may be a combination of the self-selection effect and the impact of variables of interest.

Generally, the utilization of causality analysis can be observed in different fields of study encompassing econometrics, statistics, and computer science. Drawing inspiration from these disciplines, some approaches are employed in transportation studies to address self-selection bias and evaluate policy impacts. Although these disciplines share the common goal of inferring causality, their focus and operational methodologies vary. Table 1 provides a summary of these approaches, which are widely used in transportation studies. It is worth mentioning that in epidemiology literature, significant attention has also been devoted to causality inference in the context of time-varying treatments. However, this focus diverges from the scope of our study.

Sample selection is a method used to address self-selection bias in observational studies to derive unbiased estimates in econometrics. This technique involves modelling the selection process alongside the outcome equation (Mokhtarian & van Herick, 2016). The concept of this method is built based on the Structural Equation Model (SEM) that simultaneously estimates the relationship between multiple variables and their interdependencies, which can include latent and observed variables (Golob, 2003). The standard sample selection approach consists of two equations 1) a selection equation and 2) an outcome equation which is specified based on travel behaviour indicators of interest. The Copula-based joint approach is one type of sample-selection method widely employed to model the joint distribution of multiple variables affecting decision-making processes (Parsa et al., 2019; Spissu et al., 2009). The copula approach has empowered researchers to capture a stochastic correlation among variables without being restricted by specific probability distributions. Instrumental variable (IV) is another approach used to address the potential endogeneity issue in econometrics. Endogeneity generally refers to a situation in which an explanatory variable is correlated with the error term, leading to biased estimates. In the context of causality analysis, endogeneity

Table 1: Focus of different fields of study on causality

Discipline	Approach	Focus	Limitations
Econometrics	Structural Equation Model	Captures selection process and allows for the incorporation of observed and latent variables	Depends on model specification assumption
	Copula joint approach	Captures non-linear stochastic dependencies between multiple dependent variables	Requires knowledge of joint distribution Depends on model specification assumption
	Instrumental Variable (IV)	Addresses endogeneity issues	Requires valid instruments
Statistics	Propensity Score Matching	Overcome selection bias problem	Depends on the specification of the propensity model
	Stratification		Limited to available observed covariates
	Inverse Probability Weighting		Depends on the specification of the propensity model
Computer Science	DAG-based approach	Explicitly represents causal assumptions	Requires accurate knowledge of causal structure regarding observed and unobserved variables
	Machine learning-based causal models	Captures non-linear and complex relationships in selection process	Interpretability challenges / relies on hyperparameters setting

states a broader concept where certain variables may confound the causal relationship between a policy and an outcome. In transportation studies, the Instrumental Variable (IV) method is also used (Vance & Hedel, 2007) to address endogeneity by introducing an instrument, which is a variable that is correlated with the exogenous explanatory variable, but is not directly related to the dependent variable. The instrument serves as a means to isolate the variation in the explanatory variable that is not influenced by the error term.

In statistics, based on the Rubin Causal Model (RCM), the causal effect is defined as the comparison between two potential outcomes. However, in observational studies, where both potential outcomes, related to treated and untreated conditions, are not directly observed for each individual, statisticians strive to provide comparability in the observational studies by establishing a balance between the treated and untreated (control) groups. Prominent approaches in statistics for achieving this balance include Propensity Score Matching, Inverse Probability Weighting, and Stratification. Notably, the propensity score method is a traditionally used technique in transportation studies (Cao & Fan, 2012; Cao et al., 2010). This method matches or pairs individuals with similar propensity but different policy exposure, leading to two distinct groups. After providing balance, the difference in outcome between the two groups can be attributed to the treatment, resulting in the true or causal effect of the variable of interest.

In computer science, Pearl’s Directed Acyclic Graphs (DAGs) approach and the rules of do-calculus emphasize identification rather than estimation. In observational studies, this method involves 1) causal identification and 2) converting from causality quantity to a statistical expression, known as an estimand. Interestingly, in contrast to the aforementioned methods, this approach provides us with three ladders of behavioural modelling: 1) associations analysis, 2) causation analysis by isolating the effect of confounder variables, and 3) policy effect assessment by forecasting a potential counterfactual world. In recent years, Brathwaite and Walker, 2018 discussed the

fundamental problem of the lack of using DAGs-based approaches in advanced travel behaviour models and highlighted the essential requirement of applying both causal inference and machine learning algorithms in behavioural analysis.

Inspired by the DAG-based approach, our objective is to present a comprehensive framework that addresses both causal effect analysis and the forecasting of counterfactual systems in travel behaviour modelling. Our study enjoys causal structure learning through causal discovery algorithms, utilizes structural equation models built based on the causal structure, and addresses model specification using deep learning algorithms. Notably, we leverage the capabilities of deep learning networks in predictive power while simultaneously maintaining interpretability. This study tried to initiate a new research area in causality analysis within transportation, and to the best of our knowledge, this is the first interdisciplinary effort in the context of travel behavioural modelling utilizing the advantages of traditional DCMs, deep learning algorithms and causal inference techniques.

## 2.2 Causal learning

In this section, a general overview of the main concepts of the causal discovery and causal inference method is presented. In addition, we introduce some fundamental definitions and assumptions in the causal-based analysis that can be found in previous studies and several books focusing on inferring causality (Nogueira et al., 2022; Pearl, 2009b; Peters et al., 2017; Spirtes, 2010). Causal discovery and causal inference methods are two different concepts in the causal learning discipline. Briefly, causal discovery methods infer a causal graph or causal knowledge (Shen et al., 2020), while causal inference techniques estimate the effect of a change in a certain variable, known as an intervention, on an outcome (Yao et al., 2021).

### 2.2.1 Causal discovery

The first step of inferring causality is to identify a causal structure of a system. Causal relationships between variables can be specified based on theories, domain behavioural assumptions, expert knowledge, and results of previous studies. Causal discovery is a statistical technique that is able to derive Directed Acyclic Graphs (DAGs), representing causal (in)dependencies between exogenous variables, endogenous variables and unobserved variables from observational datasets (Shen et al., 2020). Indeed, causal discovery enables us to identify non-causal associations between variables of interest in the process of modelling.

**Definition 1 (Directed Acyclic Graphs)** *A Directed Acyclic Graph (DAG),  $\mathcal{G} := (x, \zeta)$  is a graphical representation of the causal model structure, where the nodes of the graph represent random variables ( $x$ ), including exogenous variables, endogenous variables and unobserved variables, and the edges  $\zeta$  between nodes represent causal association or direct dependencies between variables. In this graphical model, the edges are directed in such a way that their direction represents the direction of causality and a node  $x_1 \in x$  is a parent ( $Pa$ ) or cause of another node  $x_2 \in x$  called child, if  $x_1 \rightarrow x_2$ . In addition, DAGs are acyclic, meaning that there are no cycles in the graph. Therefore, each DAG consists of several causal paths or directed edges pointing away from parents or ancestors ( $x_{anc}$ ) toward the child or descendants ( $x_{des}$ ).*



To learn the relationships in a DAG  $\mathcal{G}$ , there are various techniques in causal structural learning, including constraint-based, score-based, asymmetrical distribution, and hybrid approaches, differing in theories and assumptions (Nogueira et al., 2022). It is worth mentioning that in the literature, there is no standard causal discovery method and researchers usually select algorithms based on their studied problem and assumptions. Sufficiency and faithfulness are the most popular assumptions in causal discovery methods, stating that:

**Definition 2 (Sufficiency)** *There are no unobserved confounders in the causal graph  $\mathcal{G}$ , meaning that for all variables, all their causes ( $Pa_i$ ) are observed in the data.*

**Definition 3 (Faithfulness)** *Given a DAG  $\mathcal{G}$ , the faithfulness assumption states that the causal relationships that exist in the underlying causal graph accurately reflect the observed distribution among variables. This is denoted as:*

$$x_1 \perp\!\!\!\perp_{\mathcal{G}} x_2 \leftarrow x_1 \perp\!\!\!\perp_P x_2 \quad (1)$$

Faithfulness assumption allows us to infer the causal graph, by assuming all conditional independences in probability distribution  $P$  are represented in  $\mathcal{G}$ . In the following, a brief description of four causal discovery approaches is presented.

- **Constraint-based approach:** This method uses conditional independences encoded in the data to infer a graphical causal structure. Constraint-based approaches are based on the faithfulness assumption and try to identify the presence or absence of certain edges in a DAG using conditional independence tests (Nogueira et al., 2022; Spirtes et al., 2000). It is of note that faithfulness is a strong assumption that requires big sample sizes for conditional independence tests. The PC (Peter and Clark) and Fast Causal Inference (FCI) as constraint-based causal discovery approaches are widely used in the literature. The main difference between these two algorithms is that in contrast to FCI, PC makes sufficiency assumptions.
- **Score-based approach:** This algorithm evaluates the goodness of fit of a given causal model to the data and tries to optimize the goodness of fit score during learning a DAG. Score-based algorithms are also known as optimization-based algorithms. The Greedy Equivalence Search (GES) is the most popular Score-based approach starting with an empty graph and iteratively adding directed edges such that the model score like the Bayesian Information Criterion is maximized (Chickering, 2002). Fast Greedy Equivalence Search (FGES) is another modification of GES which is free from faithfulness assumption (Ramsey et al., 2017).
- **Asymmetrical Distribution-based approach:** This method is structured based on the idea that causal structure can be learned by analyzing the asymmetry in the distribution of the variables in the dataset. In other words, asymmetry is considered a fundamental characteristic of causality, and by examining these asymmetries, the method aims to uncover the underlying causal relationships. The Non-linear Additive Noise Model (NANM) and Linear Non-Gaussian Acyclic Model (LiNGAM) are classified under the asymmetrical distribution-based algorithm (Hoyer et al., 2008; Shimizu et al., 2006). Both algorithms make sufficiency assumptions. These methods are also known as functional causal models, where

LiNGAM assumes a linear relationship with non-Gaussian noise variable while NANM is specified based on a non-linear function with additive noise. These approaches involve building models in both directions and selecting the direction that satisfies the independence criterion between the cause and the noise.

- **Hybrid approach:** This approach is a combination of multiple approaches. For instance, causal Generative Neural Networks (CGNNs) as a hybrid method discover the causal relationships between multiple variables by taking into account both conditional independencies and distributional asymmetries (Goudet et al., 2018).

Broadly, DAGs provide valuable insights into the underlying causal structure of the system, enabling us to know the determining factors and confounding variables in different interventions. In order to identify confounding variables and isolate the non-causal associations or paths in the process of modelling, we need to identify a blocking set.

**Definition 4 (Blocking set)** *A blocking set  $z$  is a set of variables in a DAG that blocks or eliminates the effect of one variable  $x_1$  on another variable  $x_2$ , if either of the following conditions, shown in Figure 1, is held along their path:*

- *There is a chain structure,  $x_1 \rightarrow x_i \rightarrow x_2$  or  $x_1 \leftarrow x_i \leftarrow x_2$  and  $x_i \in z$ .*
- *There is a fork structure  $x_1 \leftarrow x_i \rightarrow x_2$  and  $x_i \in z$ .*
- *There is a collider structure,  $x_1 \rightarrow x_i \leftarrow x_2$ , and neither  $x_i$  nor any of its descendants is in  $z$ .*

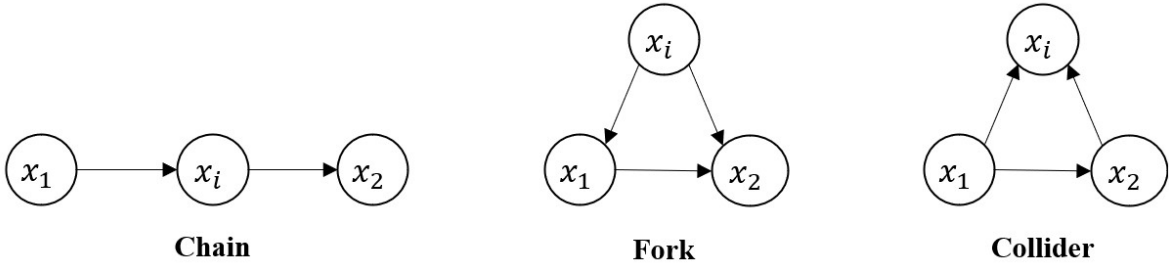


Figure 1: Three basic structures in a Directed Acyclic Graph (DAG)

After deriving the blocking set from a DAG, d-separated variables and conditional independencies can be defined as follows:

**Definition 5 (d-separated)** *Two variables are d-separated, if every path between them is blocked by a set variable known as blocking set  $z$ . In other words:*

$$(x_1 \perp\!\!\!\perp x_2) | z \quad (2)$$

This definition guides us to isolate or block any non-causal association and only keep the causal association between two variables of interest by 1) conditioning on a non-collider set and 2) not conditioning on the collider set.



### 2.2.2 Structural Causal Model (SCM)

Causal discovery is a powerful method to encode causal assumptions, but we still need to explore to what extent ‘causes’ influence ‘effects’ and how ‘interventions’ change the system. Structural Causal Models (SCM) is a type of causal inference framework that analyzes and estimates the underlying causal structures by specifying the functional relationships or causal mechanisms between variables (Pearl, 2009b). In general, each causal mechanism generates  $x_i$  given all of its causes or parents. This model structure describes how each variable in the system interacts with its causes (parents). Mathematically, in an SCM, the causal relationship of each endogenous variable with its causes or parents is specified by an asymmetrical structural equation as follows:

$$x_i := f_i(Pa_i, \beta_i) + \varepsilon_i \quad (3)$$

where  $f_i$  represents structural mechanisms, generating an endogenous variable based on causes (parents) ( $Pa_i$ ). In addition,  $\varepsilon_i$  is an exogenous latent variable representing unobserved factors or sources of variation in modelling. Estimation of the SCM involves estimating the parameters of each structural causal mechanism  $\beta_i$ . Note that equality in equations represents symmetric; However, in the causality analysis, we must put emphasis on the asymmetrical equations.

Moreover, SCMs enable the study of counterfactual scenarios in which various interventions or policies would have occurred. The counterfactual analysis allows modellers to understand how the system would behave under different changes, and make rigorous causal inferences, elaborating on the causal impact of policies before implementation. The distribution of the counterfactual world, known as intervention distribution, is the most different assumption of behavioural causal-based models compared to the prevalent behavioural frameworks.

**Definition 6 (Intervention distribution)** *An intervention distribution, mathematically denoting with the do operator  $P(Y|do(x_i))$ , refers to the probability distribution of an outcome after externally intervening in a random variable of interest  $x_i$ , known as treatment or policy.*

The intervention operation can be hard or soft as shown in Figure 2, depending on whether a variable is set to a specific value  $x_i := a$ , or whether a new structural mechanism is defined  $x_i := f'(Pa_i, \beta_i) + \varepsilon_i$

Intervention distribution conceptually is entirely different from observational distribution. In the manipulated system, the *do* operator graphically changes the causal structures in a directed acyclic graph. More precisely, regarding the causal graph, the *do* operator means all incoming links on the node variable of interest should be removed or functionality changed, and accordingly the corresponding causal mechanism should be changed in the SCM. This process results in an interventional structural causal model representing the intentional manipulation of a data-generating process. Notably the *do* or intervention operation on the variable  $x_i$  only changes the causal mechanism of  $x_i$ . This fact is rooted in the Modularity assumption or the Law of Counterfactuals, stating that in the structural causal model, causal mechanisms are modular or independent (Pearl, 2009b).

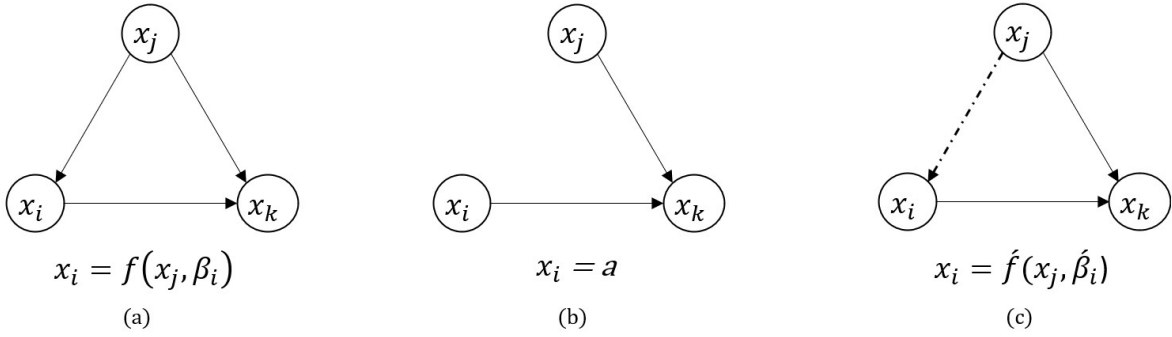


Figure 2: Visualization of Intervention Operations (a): original, (b): hard, (c): soft

### 3 Methodology

To address the inherent lack of causal inference and counterfactual analysis in advanced travel behaviour models, we introduce two model structures of our *deep CAusal infeRence mOdeling for traveL behavIour aNAlYSIS* (*CAROLINA*) framework 1) interpretable deep structural causal model, and associated 2) generative counterfactual model.

#### 3.1 Interpretable deep structural causal model

In this framework, we simultaneously capture the unobserved heterogeneity and infer causal relationships by integrating the deep neural network structure into the structural causal model in the context of Discrete Choice Models (DCMs). The structure of this framework in *deep CAusal infeRence mOdel for traveL behavIour aNAlYSIS*, (*CAROLINA*), can be found in Figure 3. Prior to modelling causal mechanisms, we need to discover a Directed Acyclic Graph (DAG), representing causal relationships between variables. In this study, we employ causal discovery algorithms to identify a DAG from observational datasets, while incorporating a certain level of domain knowledge. Generally, causal discovery is a powerful approach that allows us to infer causal relationships from observational data without prior assumptions or domain knowledge. However, it is also important to consider the constructive impact of domain-specific background knowledge in improving the causal discovery process and reducing the risk of spurious or false discoveries. In terms of DAGs searching, domain knowledge can broadly be categorized into two levels: 1) non-substantive impacts: the edges among some variables, such as socio-demographic variables should be prohibited, and 2) temporal impacts: the presence of edges from variables representing the features in the later time to those at the earlier time should be restricted (Shen et al., 2020).

In our proposed framework, *CAROLINA*, the DAG obtained from causal discovery provides the initial information for modelling causal mechanisms of utility functions in discrete choice modelling. Generally, the structural causal model is a single model that consists of a collection of asymmetrical structural equations:  $x_i := f_i(Pa_i, \beta_i) + \varepsilon_i$ . In the DAGs, random variables ( $x_i$ ) can function either purely as an exogenous variable ( $x_{ex}$ ), endogenous variable ( $x_{en}$ ) or serve the dual role of both. To construct the structural causal model, we first define the parents of all random variables.

$$Pa(x_i) = \begin{cases} \emptyset, & \text{if } \sum_{j \neq i}^n \mathbb{I}(\zeta_{ji}) = 0 \\ \{x_j, \dots, x_n\}, & \text{if } \forall x_j \setminus \{x_i\}, \mathbb{I}(\zeta_{ji}) \neq 0 \end{cases} \quad (4)$$

where, for each  $x_i$  that  $Pa(x_i) \neq \emptyset$  and  $Pa(x_i) = \{x_{ex}\}$ ,  $x_i$  is referred as the root of SCM.

In the case of DCMs, for each individual  $n$ , we start computing the utility function of  $U_{kn}$  for  $x_i$  with  $K$  discrete alternative based on causal structures.

$$\begin{aligned} U_{k_1 n}^i &=: f_{k_1}^i(Pa_{k_1 n}^i, \beta_{k_1}^i) + \varepsilon_{k_1 n}^i \\ U_{k_2 n}^i &=: f_{k_2}^i(Pa_{k_2 n}^i, \beta_{k_2}^i) + \varepsilon_{k_2 n}^i \\ &\vdots \\ U_{K n}^i &=: f_K^i(Pa_{K n}^i, \beta_K^i) + \varepsilon_{K n}^i \end{aligned} \quad (5)$$

Then, based on the probability of each alternative, the prediction of  $x_i$  is obtained and fed to the utility function of other variables that their  $Pa(x_j) = \{x_{ex}, x_i\}$ . This computation is subsequently continued until we reach the interest outcome variable or the variable playing only as a child or descendent ( $x_{des}$ ) of other variables in the causal structure.

*CAROLINA* utilizes the structure of ResNet-based models, including ResLogit and Ordinal-ResLogit, which are primarily interpretable learning-based discrete choice models for both categorical (Wong & Farooq, 2021) and ordinal (Kamal & Farooq, 2024) datasets. However, the framework is flexible enough that any other combination of interpretable models can also be used. To obtain the utility function of alternatives, first, a deterministic  $K \times 1$  utility vector is computed, where each element represents the linear impact of causes or parents ( $\beta_k Pa_{kn}$ ). This vector is then passed through  $m$  residual layers using a  $K \times K$  matrix of residual parameters  $W^m$ , resulting in the  $K \times 1$  utility vector ( $U_{kn}$ ). In this vector, each element represents the effect of  $Pa_{kn}$  on the  $k^{th}$  alternative of  $x_i$  while capturing random heterogeneity. Mathematically, the utility function of each alternative  $k$  for individual  $n$  can be obtained from Equation 6. In the following equations, for simplicity,  $i$  is eliminated from notations.

$$U_{kn} =: \beta_k Pa_{kn} + g_{kn} + \varepsilon_{kn} \quad (6)$$

In this equation, ( $g_{kn}$ ) is the heterogeneity component of residual layers which is a  $k^{th}$  element of vector  $g_n$  as follows:

$$g_n = - \sum_{m=1}^M \ln \left( 1 + \exp(W^m V_n^{(m-1)}) \right) \quad (7)$$

The residual connection comes from the previous layer and  $V_n^{(m-1)}$  is the output vector of non-linear utility components for the  $(m-1)^{th}$  residual layer consisting of  $K$  members:

$$V_n^m = V_n^{m-1} - \ln(1 + \exp(W^m V_n^{m-1})) \quad (8)$$

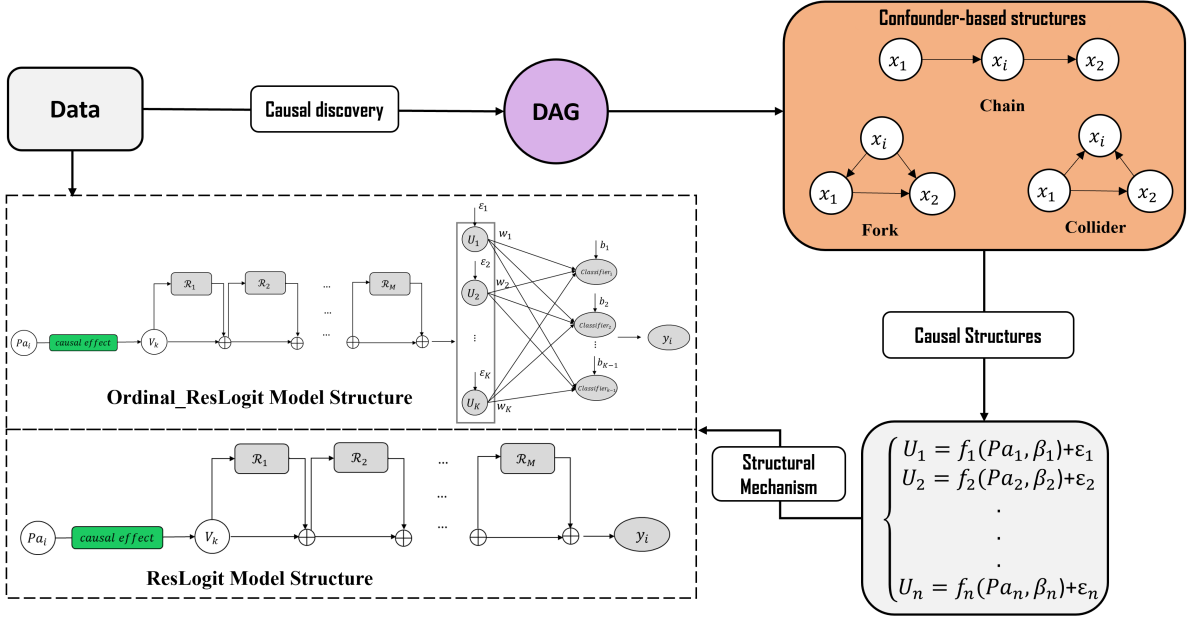


Figure 3: The architecture of interpretable deep structural causal model in *CAROLINA*

where  $V_n^0$  is the vector of linear function of parents. Then, according to the obtained utility function, for each random variable ( $x_i$ ), the probability of choosing each alternative of categorical and ordinal random variables is obtained based on the structure of ResLogit and Ordinal-ResLogit models.

$$P(x_i = k | Pa_k^i) = \begin{cases} \frac{\exp(\beta_k Pa_k^i + g_k^i)}{\exp\left(\sum_{k=1}^K \beta_k Pa_k^i + g_k^i\right)}, & \text{if } x_i : \text{Categorical} \\ \sigma\left(\left(\sum_{k=1}^K W_k(\beta_k Pa_k^i + g_k^i)\right) + b_k\right) & \text{if } x_i : \text{Ordinal} \end{cases} \quad (9)$$

where  $W_k$  and  $b_k$  are the weight and independent bias parameters of the penultimate layer of Ordinal-ResLogit in which the problem is reduced to  $K - 1$  binary classification problems. For further details on the ResLogit and Ordinal-ResLogit models, we direct the readers to Kamal and Farooq, 2024; Wong and Farooq, 2021. Based on the structural causal framework, we need to sequentially compute the effect of variables on the relevant utility function of endogenous variables based on their causal structures. The structural causal model accounts for the impact of confounders by explicitly including them in the model, resulting in isolating non-causal associations (Pearl, 2009b). Therefore, for each endogenous variable  $x_i \in x_{en}$ , the causal mechanisms modelling process involves calculating the utility functions of the random variable and determining the probability of selecting each alternative. This algorithm is mathematically presented in Appendix A.

The joint probability distribution of the variables of interest on a DAG is defined

based on the Local Markov Property and Markov Factorization property.

**Definition 7 (Local Markov property)** *A random variable  $x_i$  is independent of all its non-descendants given its parents, meaning that once we have information about the parents of variables, the variable is conditionally independent of all other random variables in the DAG that are not its descendants.*

**Definition 8 (Markov Factorization property)** *Given a probability distribution  $P$  and a directed acyclic graph  $\mathcal{G}$ ,  $P$  is factorized according to  $\mathcal{G}$ :*

$$P(x_1, \dots, x_I) = \prod_{i=1}^I P\left(x_i | Pa_i\right) \quad (10)$$

where for each causal mechanism,  $P(x_i | Pa_i)$  is specified based on the nature of random variables (categorical and ordinal) and their corresponding ResNet-based model.

In order to estimate the effect of parents ( $\beta$ ) and total deep layers parameters ( $\theta$ ) including residual layers and the penultimate layer of Ordinal-ResLogit, all causal mechanisms are jointly modelled, and the loss function shown in Equation 11 is minimized by using a minibatch data-driven stochastic gradient descent-based (SGD) learning algorithm an RMSprop optimization step (Goodfellow et al., 2016).

$$LL(\beta, \theta) = \sum_{n=1}^N \sum_{i=1}^I \left[ \ln(P(x_1, \dots, x_I) M_n) \right] \quad (11)$$

where  $M_n \in \{0, 1\}$  is the chosen alternative among joint alternative of interest. In the context of prediction, the predicted values of the parents in the causal structure are fed into the utility function of their corresponding child variable.

### 3.2 Counterfactual model structure

The intervention distribution or counterfactual world is not observable in the present. The counterfactual distribution (*do* operator) represents how the outcome may change if the policies or external intervention are externally implemented (Pearl, 2009a, 2009b; Shpitser & Pearl, 2006). To estimate the true causal effects of interventions, we often require the model of human behaviour in the counterfactual world, leading to generating a counterfactual distribution. The counterfactual model is based on the current causal structure, where some causal mechanisms are changed, but the latent variables remain unchanged (Pearl, 2009b; Peters et al., 2017). The counterfactual model is a unit-level analysis that allows us to predict counterfactual outcomes under different intervention scenarios and compare them with observed outcomes. In other words, the counterfactual model structure assists us in making inferences about how individuals would have changed their decisions if transportation planners had intervened in the system. Therefore, we are able to compute both the true causal interventions and individual treatment effects. A typical counterfactual modelling process consists of three levels: abduction, manipulation, and prediction (Pearl, 2009b). These steps are clarified and visualized in Figure 14 in Appendix B. The figure also compares the counterfactual prediction model with the classic forecasting approach. In contrast to the association-based model, our

proposed model initially endeavours to learn how the observed variables relate. Subsequently, upon learning the latent structure, the model predicts the impact of policy changes by considering alterations in the causal mechanisms

First, the abduction step is required in order to infer the latent exogenous variables of each causal mechanism  $P(\varepsilon_i|x_i)$  where  $x_i$  represents the exogenous variable of the mechanism. This step helps us to understand the uncertainty and variability in the system that is assumed to be identical to the counterfactual world. To clarify this, let us focus on one part of an obtained DAG shown in Figure 4. In this example,  $Pa(x_A) = \{Pa_A^1, Pa_A^2, \dots, Pa_A^n\}$  are parents set of a discrete binary random variable  $x_A$  and for this part of DAG the causal mechanism associated to the utility function of this variable is  $U_A =: f_A(Pa_A, \beta_A) + \varepsilon_A$ . At the abduction level, we aim to approximate  $\varepsilon_A$  that is behind the generation of the endogenous variable. This variable is known as the latent or unobserved variable.

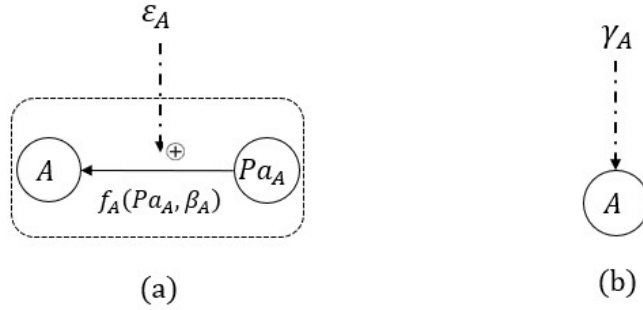


Figure 4: The visualization of latent construct in a DAG

To capture a more accurate approximation of the latent construct, we leverage the capabilities of both the Variational Auto Encoder (VAE) and normalizing flow. In the context of posterior distribution inference, VAE has been used in various disciplines to learn a latent space that captures the underlying factors of variation in the observed data (Kingma & Welling, 2019). The VAE consists of an encoder network that maps the observed data  $x_i$  to a latent space representation, and a decoder network that reconstructs the data from the encoded compression of  $x_i$ . In other words, the encoder network parameterizes the approximate posterior distribution  $P(\varepsilon_i|x_i)$ , while the decoder network models the conditional distribution  $P(x_i|\varepsilon_i)$ . Therefore, in the inference stage, given observed data  $x_i$ , the encoder network can be used to obtain a sample from the approximate posterior distribution  $P(\varepsilon_i|x_i)$ . The VAE traditionally assumes a simple distribution, such as a Gaussian distribution, for the latent space. However, this assumption may constrain the ability of model to infer an expressive posterior distribution and approximate a flexible enough distribution that accurately represents the underlying latent space of observed variables.

By incorporating the Normalizing Flow technique into the VAE, we can flexibly transform the simple distribution into a more representative distribution (Kingma et al., 2016). Generally, the normalizing flow model is a powerful generative modelling technique that allows for the flexible transformation of a simple base distribution to a more complex distribution (Kobyzev et al., 2020; Papamakarios et al., 2021). In the literature, although the wide use of normalizing flows is to perform density estima-



tion, flows-based models have emerged as a powerful tool for posterior approximations (Papamakarios et al., 2021).

Our Flow-based VAE framework involves learning the latent space representation of the exogenous variables or input of a causal mechanism notated by  $\gamma_i$ . As shown in Figure 4, we assume another form of causal mechanism generating process, depending on the compressed latent representation of the observed variables, and by comparing both structures, the  $\varepsilon_i$  is computed as:

$$\varepsilon_i = \gamma_i - f_i(Pa_i, \beta_i) \quad (12)$$

To learn the  $\gamma_i$ , the Flow-based VAE framework consists of three structures, encoder, normalizing flow model, and decoder. In our study, we use two MultiLayer Perceptron (MLP) structures for modelling the encoder and decoder of the VAE. First, based on causal mechanisms obtained from the DAG, the encoder structure takes observed exogenous data ( $x_i$ ) and generates the mean ( $\mu$ ) and standard deviation ( $\sigma$ ) of the initial variable of the flow model. The reparameterization process is used to set the simple standard Gaussian distribution as a base distribution of latent variable  $\gamma_0 \sim \mathcal{N}(\gamma_0|\mu, \sigma^2)$  (Rezende & Mohamed, 2015). The  $\gamma_0$  value is then fed into the first flow layer. Normalizing flow structures consist of a stack of flow layers and transform the simple distribution into a distribution which is more representative of the true underlying distribution ( $Q_k(\gamma_k)$ ). In fact, in the abduction level, both the encoder and normalizing flow model are used to infer latent constructs. Note that  $\gamma_k$  is the latent space representation of observed variables of the causal mechanism and can be computed as:

$$\gamma_k = h_k \circ h_{k-1} \circ \dots \circ h_1(\gamma_0) \quad (13)$$

The distribution of the last variable equals the product of absolute values of determinants of Jacobin for each transformation (Kobyzev et al., 2020; Papamakarios et al., 2021; Rezende & Mohamed, 2015).

$$Q_k(\gamma_k) = Q_0(\gamma_0) \prod_{k=1}^k \left| \det \frac{\partial h_k}{\partial \gamma_{k-1}} \right|^{-1} \quad (14)$$

In Equation 14, the determinant term is computationally expensive; however, in our study, we use Planar flow to control the efficiency of the model (Kobyzev et al., 2020; Rezende & Mohamed, 2015). The formula for this transformation is written as follows:

$$h(\gamma) = \gamma + uh(w^T \gamma + b) \quad (15)$$

where  $u$ ,  $w$  and  $b$  are learnable parameters of the normalizing flow structures. Finally, the decoder takes the latent variable ( $\gamma_k$ ) and models the observed variables. The algorithm of the counterfactual model structure is also mathematically presented in Appendix 1.

To train the Flow-based VAE model, we simultaneously estimate the set of parameters of encoder and normalizing flows ( $\phi$ ) and also decoder parameters ( $\psi$ ) by minimizing the negative lower bound of log-likelihood called Evidence Lower Bound (ELBO).

ELBO consists of two terms: 1) Kullback–Leibler(KL) divergence between the approximate posterior and the actual distribution, and 2) reconstruction error (Rezende & Mohamed, 2015). The negative ELBO can be computed as:

$$-ELBO(\phi, \psi) = KL\left[Q_\phi(\gamma|Pa_i)||P_\psi(\gamma)\right] - \mathbb{E}_{Q_\phi(\gamma|Pa_i)}\left[\log P_\psi(Pa_i|\gamma)\right] \quad (16)$$

where the KL divergence is:

$$KL\left[Q_\phi(\gamma|Pa_i)||P_\psi(\gamma)\right] = \mathbb{E}\left[\log Q_\phi(\gamma|Pa_i)\right] - \mathbb{E}\left[\log P_\psi(\gamma)\right] \quad (17)$$

Therefore, the Equation 17 can be written as:

$$-ELBO(\phi, \psi) = \mathbb{E}_{Q_\phi(\gamma|Pa_i)}\left[\log Q_\phi(\gamma|Pa_i) - \log P_\psi(Pa_i, \gamma)\right] \quad (18)$$

Given three components of the flow-based VAE model and parametrization technique, the negative ELBO is obtained as follows (Rezende & Mohamed, 2015):

$$-ELBO(\phi, \psi) = \mathbb{E}_{Q_0(\gamma_0)}\left[\log Q_k(\gamma_k) - \log P(Pa_i, \gamma_k)\right] \quad (19)$$

and finally, by substituting 14, the loss function can be computed as:

$$-ELBO(\phi, \psi) = \mathbb{E}_{Q_0(\gamma_0)}\left[\log Q_0(\gamma_0)\right] - \mathbb{E}_{Q_0(\gamma_0)}\left[\sum_{k=1}^K \log \left| \det \frac{\partial h_k}{\partial \gamma_{k-1}} \right| \right] - \mathbb{E}_{Q_0(\gamma_0)}\left[\log P(Pa_i, \gamma_k)\right] \quad (20)$$

Minimizing this loss function with respect to  $\phi$  and  $\psi$  ensures the optimization of both the variational inference and generative components of the model. As observed in Equation 16, a small KL divergence results in a tighter ELBO, which serves as a superior lower bound for  $\log P_\psi(Pa_i)$ , resulting in unbiased generative model parameters. Furthermore, through the utilization of normalizing flow, we try to minimize KL divergence and enhance the flexibility of the encoder component in the VAE. Consequently, optimizing the Equation 20 not only ensures a reduction in KL divergence but also enhances the performance of the generative model.

In our study, we adapt the Flow-based VAE framework for the utility function of discrete variables of interest. After completing the abduction level and estimating the latent variables, in order to predict counterfactual outcomes, we need to develop the interventional deep SCM, representing the manipulated system. This step involves specifying the intervention(s) or policy and manipulating the causal mechanism either in the soft or hard operation, shown in Figure 2. In this study, we manipulate the system based on the soft operation and we define the chosen intervention according to our research question and the desired causal effect to be estimated. Eventually, the interventional model structure can be used to predict the counterfactual outcome and the effect of the intervention. The complete structure of our proposed counterfactual model consisting of abduction, manipulation, and prediction is illustrated in Figure 5 and the algorithm of our proposed model can be found in Appendix A.

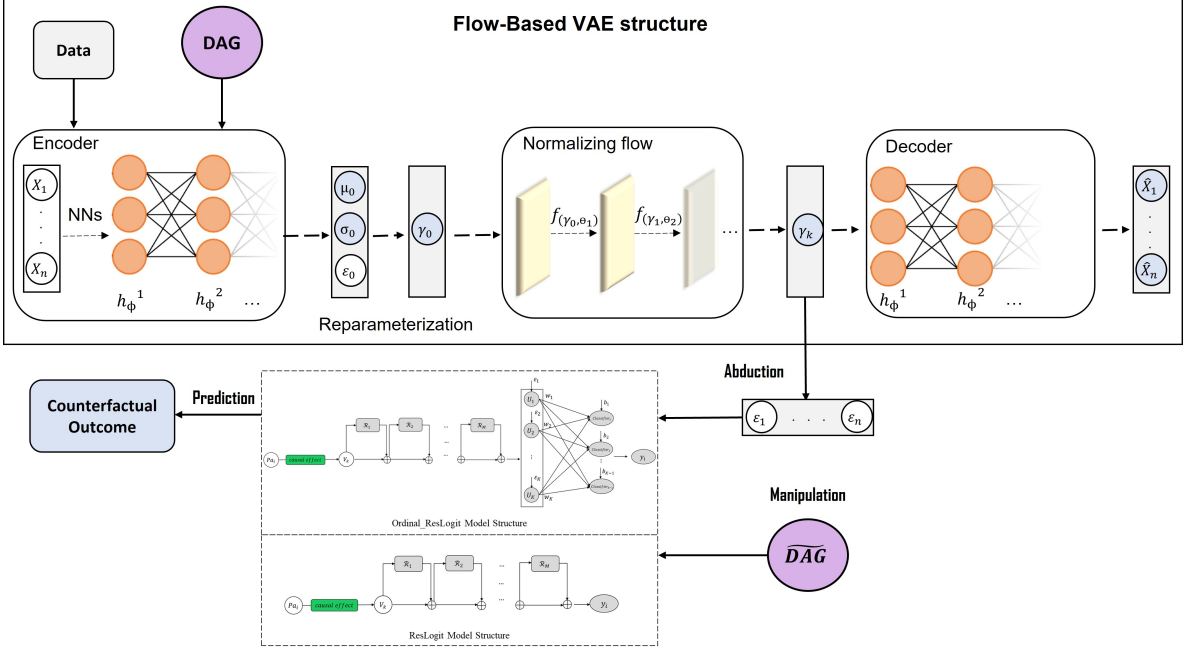


Figure 5: The architecture of generative counterfactual model in *CAROLINA*

## 4 Case Studies

For a comprehensive analysis, we use two observational datasets: 1) a pedestrian crossing behaviour dataset collected based on Virtual Immersive Reality Experiment (VIRE) (Farooq et al., 2018) in a controlled environment, and 2) a revealed preference for travel behaviour in London. Moreover, a synthetic dataset is also generated with ground truth to analyze the properties of the proposed framework.

### 4.1 Data

The first dataset consists of 1,406 responses for pedestrian crossing behaviour under different scenarios involving interactions with current traffic conditions, fully automated vehicles, and mixed traffic conditions (Mudassar et al., 2022). These scenarios were defined based on various controlled factors presented in Table 2. In addition, Galvanic Skin Response (GSR) sensors were utilized during the experiments to measure the relative stress levels of the participants. The GSR sensor uses a small electrical charge to measure the amount of sweat on an individual’s finger, where a higher charge indicates greater sweat production. It is important to note that in our study the mean stress level of pedestrians in each scenario was normalized based on their minimum and maximum observed stress levels within that scenario. Detailed information on the scenario definitions can be found in Mudassar et al., 2022.

Moreover, we use an openly available dataset, the London Travel Demand Survey (LTDS), to investigate the travel demand in the metropolitan area of London (Hillel et al., 2018). This dataset combines the individual trip records from April 2012 to March 2015 with corresponding trip trajectories and mode alternatives obtained from a directions Application Programming Interface (API). Our focus in this study is on non-

Table 2: Description of explanatory variables of pedestrian crossing behaviour

Variable	Description	Mean	Standard deviation
<b><i>Street Characteristics</i></b>			
lane Width			
Low	1: If the lane width is less than 2.75 meter, 0:otherwise	0.334	0.472
Medium	1: if the lane width equals to 2.75 meter, 0: otherwise	0.307	0.462
High	1: If the lane width is greater than 2.75 meter, 0:otherwise	0.359	0.480
Road Type			
Two way with a median	1: If the road type is two way with median, 0:otherwise	0.338	0.473
Two way	1: If the road type is two way, 0:otherwise	0.317	0.466
One way	1: If the road type is one way, 0:otherwise	0.344	0.475
Traffic Density	Density of road (veh/hr/ln)	19.835	7.158
<b><i>Traffic Condition</i></b>			
Automated Condition			
Mixed	1: If traffic in scenario consists of automated vehicles and human-driven vehicles, 0:otherwise	0.045	0.207
Fully automated	1: If traffic in scenario consists of only automated vehicles, 0:otherwise	0.925	0.263
Human-driven condition	1: If traffic in scenario consists of only human-driven vehicles, 0:otherwise	0.029	0.170
<b><i>Socio-demographic</i></b>			
Age group			
18-25	1: If participant' age is between 18 and 30, 0:otherwise	0.542	0.498
25-39	1: If participant' age is between 30 and 39, 0:otherwise	0.339	0.474
40-49	1: If participant' age is between 40 and 49, 0:otherwise	0.034	0.182
Over 50	1: If participant' age is more than 50, 0:otherwise	0.084	0.278
Gender	1: If participant is female, 0:otherwise	0.382	0.486
Driving Licence	1: If participant has a driving license, 0:otherwise	0.895	0.307
Car Access			
No car	1: If participant has no car in the household, 0:otherwise	0.302	0.345
One car	1: If participant has one car in the household, 0:otherwise	0.345	0.476
Over one car	1: If participant has more than one car in the household, 0:otherwise	0.353	0.478
Travel Mode			
Active mode	1: If participant use active modes regularly, 0:otherwise	0.258	0.438
Private car mode	1:If participant use private car regularly, 0:otherwise	0.332	0.471
Public mode	1: If participant use transit regularly, 0:otherwise	0.409	0.492
<b><i>Crossing Attributes</i></b>			
Wait Time	High: If participant's Wait Time on the sidewalk is greater than 5 seconds, Low: otherwise	0.357	0.479
Stress Level	High: If participant's normalized stress is greater than 0.59, Low: otherwise	0.252	0.435
<b><i>Environment Condition</i></b>			
Night	1: If the time of scenario is night, 0:otherwise	0.371	0.483
Snowy	1: If the weather of scenario is snowy, 0:otherwise	0.293	0.455

mandatory trips, where individuals have flexibility in selecting their destination based on their preferences and trip characteristics. Table 3 presents a list of explanatory variables used in this study.

It is worth mentioning that in this study, pedestrian wait time, stress level and

travel distance variables are discretized into discrete categories using Jenks Natural Breaks classification method (Jiang, 2013). This method categorizes a given dataset into multiple categories, with the objective of minimizing the variance within each group and maximizing the variance between different groups. The optimum thresholds of different categories for these variables are presented in Table 2 and 3.

Table 3: Description of explanatory variables of London travel behaviour dataset

Variable	Description	Mean	Standard deviation
<b><i>Travel Attributes</i></b>			
Travel Mode			
Private car	1: if individual uses private car, 0: otherwise	0.478	0.450
Public transit	1: if individual uses public transportation, 0: otherwise	0.296	0.456
Active modes	1: if individual uses bike or walking, 0: otherwise	0.226	0.456
Travel Cost			
Transit cost	Travel cost for transit mode (£)	1.456	1.287
Driving cost	Total travel cost for private car mode (£)	1.423	2.853
Travel Distance	Long: more than 7.8 kilometers away from their starting point, Medium: otherwise	0.529	0.499
<b><i>Socio-demographic</i></b>			
Age Group			
18-30	1: if individual's age is between 18 and 30, 0: otherwise	0.185	0.388
30-45	1: if individual's age is between 30 and 45, 0: otherwise	0.315	0.465
45-60	1: if individual's age is between 45 and 60, 0: otherwise	0.232	0.422
Over 60	1: if individual's age is more than 60, 0: otherwise	0.268	0.443
Gender	1: if individual is female, 0: otherwise	0.557	0.497
Disability	1: If participant has a driving license, 0: otherwise	0.895	0.307
Driving License	1: if individual has a driving license, 0: otherwise	0.718	0.450
Unrestricted Car Access	1: if there is one or more than one car in the household, 0: otherwise	0.271	0.444

## 4.2 Model hyperparameters

In the context of deep learning, the model hyperparameter setting plays an important role in determining the performance and generalization capabilities of the model. In the process of modelling, we divided the dataset into two subsets using a 70:30 training/validation split. In this study, we employ the random search technique to optimize the hyperparameters of our model. This involves defining a range of values for each hyperparameter and randomly selecting combinations from these ranges to train the model on the training dataset (Bergstra & Bengio, 2012). Table 4 shows the range of hyperparameters used in the random search method.

Note that in this study we use the early-stopping approach to overcome the overfitting problem; however, regularization techniques, that may further enhance the performance of learning models, are not used in our study. This decision was made to facilitate a fair comparison between our proposed model and econometric models. We implement the structure of our proposed model using open-source deep learning libraries

in Python. The code for our experiments will be available on the lab’s GitHub as the manuscript is published.

Table 4: Range of model hyperparameters

Parameters	Value
Residual Layers	{2, 4, 8, 16, 32}
Learning rate	{0.01, 0.001}
Batch size	{32, 64}
Number of hidden layers	{4, 6}
Threshold of ordinal categories	[0.3, 0.6]

## 5 Results and Discussion

This section is divided into three subsections in which the results of causal discovery, interpretable deep structural causal modelling, and the generative counterfactual model for each dataset are provided.

### 5.1 Directed Acyclic Graphs (DAGs) Learning

In order to learn Directed Acyclic Graphs (DAGs) for each dataset, we focus on the causal discovery algorithms that are based on sufficiency assumptions, meaning that the observed data contains sufficient information to determine the causal relationships between variables. In other words, we assume that the causal graphs are not influenced by any unobserved confounders. PC and FGES described in Section 2.2.1 are two popular causal discovery algorithms based on sufficiency assumptions; nevertheless, in the literature, there is no standard causal discovery method. In this study, we choose the FGES algorithm for two reasons. The FGES enjoys parallelization techniques in optimization and searching the causal graph. In addition, although the PC algorithm and its variants consist of two phases: searching a skeleton and orienting the edges, they are not appropriate for big datasets as the second phase may be removed, resulting in an undirected graph (Nogueira et al., 2022).

#### 5.1.1 Pedestrian crossing behaviour

To learn the causal structures of pedestrian behaviour in the presence of automated vehicles, the following prior knowledge is considered:

- The street characteristics, traffic condition, and environment condition variables are only allowed to cause changes in pedestrian wait time and stress level.



- The meaningless relationship between some socio-demographic variables like age  $\rightarrow$  gender or driving licence  $\rightarrow$  age are prohibited. However, the logical cause and effect relationships such as age  $\rightarrow$  driving licence are allowed.

Figure 6 illustrates the causal structure obtained from FGES algorithm for the pedestrian crossing behaviour. Interestingly, this causal structure confirms our assumption in previous studies stating that pedestrian stress level influences their waiting time (Kamal & Farooq, 2022). Furthermore, a first glance at this graph illuminates our needs in causality analysis. In fact, in most travel behaviour analyses in transportation, we assume all observed variables as contributing factors of outcome and wrongly interpret significant associations as the likely reasons for changes in the outcome. However, this assumption would not be representative of the true behaviour-generating process. For instance, in the causal structures of pedestrian behaviour, there is no direct relationship between the number of cars in the household and pedestrian wait time. However, the result shows the number of cars directly influences pedestrian stress level and thus the effect of this variable is transferred to pedestrian wait time through their stress level. Conversely, in typical behavioural modelling in transportation, by conditioning on both the number of cars and stress level variables, the indirect effect of the number of cars on pedestrian waiting time is blocked and can not be estimated.

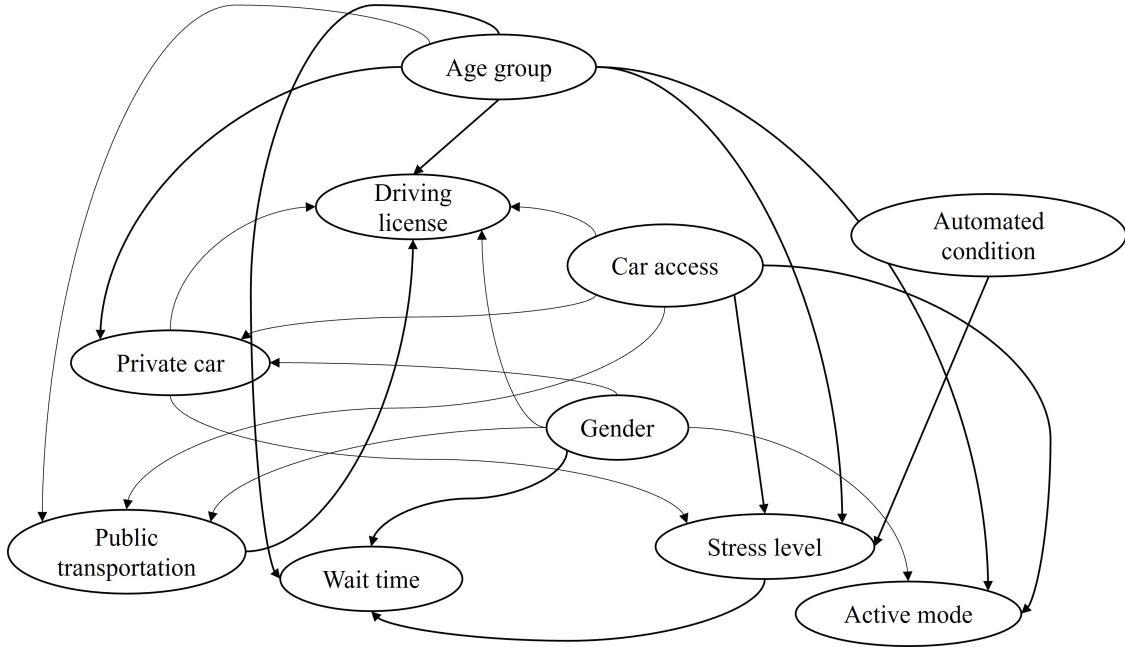


Figure 6: Causal structure of pedestrian crossing behaviour

In this causal graph, age, gender, number of cars and traffic condition are only exogenous variables and other variables play roles as both exogenous ( $x_{ex}$ ) and endogenous ( $x_{en}$ ) variables in our framework. Our interest is in the causal effect of pedestrian stress level (policy) on the waiting time (outcome) (stress level  $\rightarrow$  waiting time). As shown in Figure 6, between these variables, the fork structure can be observed due to peoples' age. In other words, this variable is the common cause of generating waiting time and stress level, potentially confounding the true impact of variables on each other. These

findings underscore the vital importance of identifying causal structures in behavioural modelling, particularly in the study of policy assessment.

### 5.1.2 London travel behaviour

Figure 7 demonstrates the behaviour-generating process in the London travel dataset obtained from the FGES algorithm. For this dataset, we also contemplate the following prior knowledge:

- Regarding some socio-demographic variables such as age, gender, disability and car access variables are treated to be exogenous variables ( $x_{ex}$ ) in the model. In other words, these variables are not affected by any other variable (parents) in the causal structures.
- The meaningless relationships between some socio-demographic variables like age  $\rightarrow$  gender are not allowed.
- Any direct connection between travel modes, including private car, public transit, and active modes, is prohibited. Note that in the modelling the cross-effect of mode choices is captured by using deep residual layers.
- The connection between an alternative and non-alternative-specific attributes (attributes of other travel modes) is restricted.
- The cost of both driving and transit are not allowed to be influenced by any other variables in this dataset.

The results uncover that for non-mandatory trips, the arbitrary choice of travel distance is a cause of the choice of travel modes. However, other common causes between these two variables may also connect them through a non-causal path. This result does not mean that our study criticizes the previous studies in which researchers evaluated the effect of travel mode choice on travel distance. Such variations might arise due to two reasons. First, each causal structure describes one population, implying that causal graphs of similar problems should be localized for each population (Pearl, 2009b). Secondly, unlike previous studies that emphasized association-based analysis, we prioritize causality analysis for policy assessment. The non-causal studies are able to reveal associations between variables, however, these associations must not be interpreted as causal associations or used for policy assessment. In the next section, in order to model the causal direction between travel distance (policy) and three travel modes (outcome), we extract endogenous and related exogenous variables and build the structural causal model based on this causal structure.

## 5.2 Cause and Effect Analysis

The causal graphs obtained from the discovery process are fed into the deep structural causal model of *CAROLINA*. This model structure is able to jointly model the causal mechanisms of discrete variables, both categorical and ordinal. To compare the performance of *CAROLINA*, we also developed a conventional structural causal model (SCM-Logit) for both datasets. This model is built on Multinomial Logit (MNL) and

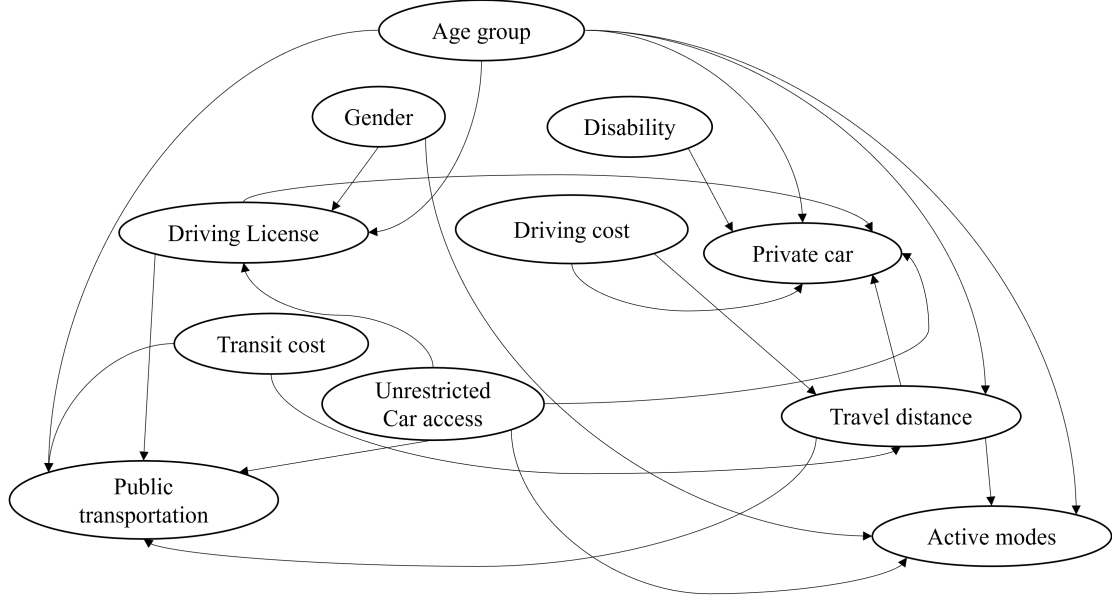


Figure 7: Causal structure of London travel behaviour

Ordered Logit Models that are widely used in the literature. It is noteworthy that our previous research has already undertaken comparisons between these conventional discrete choice models and the corresponding ResNet-based model structures (Kamal & Farooq, 2024; Wong & Farooq, 2021). In the current study, we extend this analysis by applying these models to the task of modelling causal structures. Our preliminary assumption is that both *CAROLINA* and SCM-Logit are based on the causal structures obtained from DAGs and the only difference between models is the modelling of parent-child relationships.

In the study of pedestrian crossing behaviour, in order to estimate the causal link between stress level and pedestrian wait times, our model approach takes into account the causal relationship between travel mode choice, pedestrian stress level, waiting time and other exogenous variables. In fact, based on the causal structure, for instance, an individual’s inclination towards private car usage may impact their stress levels on a sidewalk. Concerning the second dataset, we analyze the causal process in which individuals choose medium and long travel distances and examine how these choices, along with their possession of a driving license, directly influence their travel behaviour. Table 5 and 6 present the results obtained for pedestrian crossing and travel behaviour datasets respectively.

Since the total number of parameters/weights associated with the deep layers proportionally increases due to the underlying neural network structure, for the model selection and analysis of the goodness of fit, we used the Akaike Information Criterion (AIC) values (Equation 21) to compare the two model structures.

$$AIC = -2LL(\beta, \theta) + 2B \quad (21)$$

The lower AIC value of *CAROLINA* compared to the SCM-Logit in Table 5 shows that *CAROLINA* is able to capture the underlying data-generating process better.

Table 5: Results of estimated models for pedestrian crossing dataset

Exogenous	Endogenous			
	CAROLINA		SCM-Logit	
	Travel Mode Choice			
	Public Transit	Active	Public Transit	Active
Age 25-29	0.950 (6.530*)	0.218 (0.985)	-0.380 (-2.152)	-0.242 (-1.008)
Age 30-39	-0.177 (-1.724)	-	-	-
Age over 50	-0.419 (-1.869)	-0.812 (-2.290)	-0.279 (-0.936)	-
Gender	1.227 (6.750)	1.125 (4.754)	0.919 (7.045)	0.316 (1.590)
One car	-	-0.548 (-3.549)	-0.905 (-6.850)	-0.464 (-2.520)
Over one car	-0.776 (-7.366)	-0.560 (-3.571)	-0.805 (-5.976)	-0.431(-2.328)
Stress Level				
Age 25-29	-		0.235 (1.429)	
Age 30-39	0.991 (2.579)		-0.491 (-3.832)	
Age 40-49	-		-	
Age over 50	0.949 (1.005)		-	
One car	0.356 (1.697)		0.268 (1.985)	
Over one car	0.395 (1.789)		-	
Private car	0.083 (2.859)		-1.354 (-8.496)	
Fully automated condition	0.539 (2.346)		0.307 (3.693)	
Mixed Traffic condition	-0.037 (-0.916)		-	
Wait time				
Age 25-29	-		-	
Age 30-39	1.056 (5.406)		-0.088 (-1.860)	
Age 40-49	-		-	
Age over 50	-		-0.284 (-1.166)	
Gender	0.770 (5.862)		0.205 (1.836)	
Stress level	0.843 (5.154)		-0.111 (-0.878)	
No. observation	1406		1406	
No. parameters	300		16	
Log-likelihood	-1342.01		-1833.13	
AIC	3284.02		3698.26	
Mean Prediction Error (MPE)				
Travel Mode	29.94%		49.36%	
Stress Level	21.34%		54.78%	
Wait time	41.08%		44.90%	

\* t-stats are outlined in the parenthesis.

In addition, concerning the accuracy, we use Mean Prediction Error (MPE) on the validation dataset:

$$MPE = \frac{1}{N} \sum_{n=1}^N \mathbb{I}(y_n \neq \tilde{y}_n) \quad (22)$$

where  $y_n$  and  $\tilde{y}_n$  are the actual and predicted choices for each individual  $n$  and indicator index  $\mathbb{I}$  equals 1 when the expression inside is true and otherwise, it is 0. In terms of pedestrian crossing behaviour, we observe approximately 19.4% and 33.4% and 3.8% differences in the accuracy of discrete travel mode choice, stress level, and waiting time causal mechanisms respectively. Furthermore, in the travel behaviour data, a notable improvement in the accuracy of model is observed by 27.2% in the prediction of travel distance. These values in prediction highlighted the effective role of the deep learning part of our proposed model, allowing for capturing unobserved heterogeneity from data. The impacts of significant exogenous variables in causal mechanisms are also shown in Table 5 and 6 with t-statistic information. In terms of variable selection in the modelling, the distinguishable distinction between our approach and previous transportation studies is that in our models, each causal mechanism only takes variables identified as their parent or causal factors within the causal structure.

Concerning pedestrian crossing behaviour, our result reveals that daily using private cars positively causes pedestrian stress levels. In fact, among other alternatives, the habitual use of private cars significantly influences the level of stress experienced by individuals on the sidewalk. Another noteworthy result of the pedestrian crossing study shows that their stress level significantly changes their decisions regarding the start time of crossing. In other words, a high level of stress, which can be influenced by pedestrians' age group, gender, travel pattern, and traffic conditions, results in longer waiting time on the sidewalk. However, the reverse is obtained in the SCM-Logit. This outcome contradicts our real-world expectations. In fact, typically, individuals experiencing stress are expected to hesitate to cross the street immediately and wait longer on the sidewalk. It is worth noting that regarding road-related attributes our causal discovery approach only reveals relationships between road-related attributes and the stress level. The same result is also obtained by using PC algorithm. However, it is important to acknowledge that due to the limitations of the virtual reality dataset, further research is necessary to validate and expand upon any direction between other road-related attributes and stress level or the duration of waiting time on the sidewalk.

Regarding the travel behaviour dataset, our findings indicate that increased household accessibility to private cars correlates with a higher probability of possessing a driving license. Subsequently, individuals with driving licenses demonstrate a stronger preference for both private cars and public transportation, although the inclination towards private cars is significantly higher. However, according to SCM-logit analysis, having a driving license likely leads to a greater inclination towards active modes of transportation compared to public transportation. Furthermore, we specifically evaluate the direct impact of travel distance on people's preference towards travel modes. Indeed, the DAG indicates the direction between these variables. The opposite direction may also exist, but the confounding variables serve as the primary reason for this direction, rather than a true cause and effect. Our result demonstrates that choosing more distant destinations for non-mandatory trips negatively changes the probability of

Table 6: Results of estimated models for travel behaviour dataset

Exogenous	Endogenous			
	<i>CAROLINA</i>		SCM-Logit	
Driving Licence				
Female	-1.006 (-2.339)		-0.207 (-3.550)	
Age 30-45	1.325 (2.321)		0.287 (3.776)	
Age 45-60	1.455 (1.941)		0.302 (2.459)	
Age over 60	0.755 (1.055)		0.153 (6.956)	
Unrestricted Car Access	5.839 (1.915)		0.568 (4.501)	
Travel Distance				
Age 30-45	-0.015 (-4.442)		-0.072 (-3.385)	
Age 45-60	-0.045 (-11.461)		-0.080 (-3.243)	
Age over 60	-0.157 (-5.827)		0.227 (10.239)	
Transit cost	-0.011 (-8.197)		0.218 (6.343)	
Driving cost	1.664 (6.784)		0.058 (16.196)	
Travel Mode Choice				
	<i>Public Transit</i>	<i>Private Car</i>	<i>Public Transit</i>	<i>Private Car</i>
Age 30-45	-0.070 (-3.971)	0.346 (1.371)	-0.114 (-5.002)	-0.146 (-6.976)
Age 45-60	-0.196 (-8.460)	0.370 (1.046)	-0.116 (-4.173)	-0.076 (-3.152)
Age over 60	-0.828 (-2.282)	-0.217 (-12.059)	0.129 (5.081)	-0.064 (-2.837)
Disability	-	-0.647 (-10.731)	-	-0.245 (-4.705)
Driving Licence	0.104 (7.332)	1.775 (5.329)	-0.302 (-2.786)	0.262 (9.497)
Driving cost	-	-0.438 (-2.681)	-	-0.060 (-4.651)
Transit cost	-0.156 (-1.159)	-	0.013 (2.0553)	-
Unrestricted Car Access	-0.365 (-3.304)	0.942 (1.458)	-0.092 (-3.498)	0.277 (12.858)
Long Travel Distance	-1.442 (-4.051)	0.433 (1.064)	0.685 (4.148)	0.522 (3.232)
No. observation	45,547		45,547	
No. parameters	299		26	
Log-likelihood	-47,055.94		-70,701.37	
AIC	94,709.88		141,454.74	
Mean Prediction Error (MPE)				
Driving Licence	26.94%		27.87%	
Travel Distance	10.87%		38.10%	
Travel Modes	36.96%		39.54%	

\* t-stats are outlined in the parenthesis.



opting for public transportation and increases people’s tendency towards using private cars. In other words, in the travel behaviour-generating process, as the distance of the trip increases, there is a corresponding decrease in the individual’s propensity towards modes of transportation that are environmentally friendly and promote sustainability. However, based on our study, we are not allowed to mistakenly conclude that choosing a private car leads to a further destination. This is a key distinction between our analysis and previous efforts in the transportation literature.

*CAROLINA* can be as complete as the traditional econometric models in terms of calculating the elasticity, substitution patterns and other economic information. Despite using deep layers, our framework benefits from the key components of discrete choice models, extracting the economic information using an interpretable utility function. The Resnet-based models ensure the monotonicity of the marginal utilities. This is substantiated by Figure 8, which illustrates that in London travel behaviour, as the travel cost of each alternative increases, the corresponding utility function decreases. Furthermore, our framework enables us to confine the utility function of each alternative solely to its attributes, ensuring alternative-specific attributes assumption in the model specification. To show the capability of our model in extracting behavioural indicators, we use the substitution pattern information to demonstrate how the choice probability of alternatives shifts in response to changes in a direct effect of a targeting variable, while keeping other influences constant. Figure 9 illustrates the impact of driving costs on the choice probability concerning travel distance and travel model discrete choices.

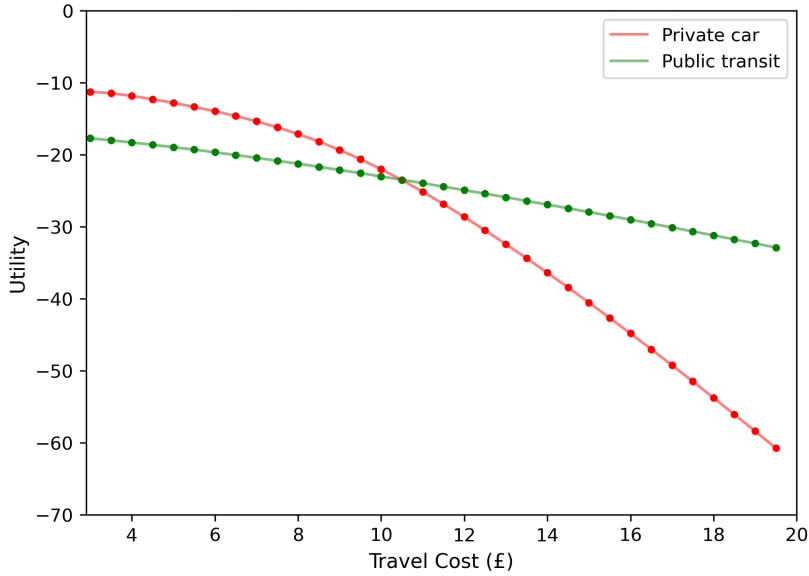


Figure 8: Utility contributions in London travel behaviour dataset

Figure 9 illustrates that as the driving cost increases, the inclination towards selecting recreational destinations gradually shifts towards more distant locations in such a way that reaching approximately a driving cost of £16, the medium-distance category emerges as a substitute for longer travel distances. Interestingly, our results also indicate that when the driving cost is less than £2.5, individuals are more inclined towards opting for private car transportation in London. However, this inclination gradually

changes to a preference for public transit. In fact, as the driving cost increases, there is a discernible shift in people’s travel patterns in London, transitioning from long-distance travel to medium-distance travel, accompanied by a notable preference shift towards public transportation.

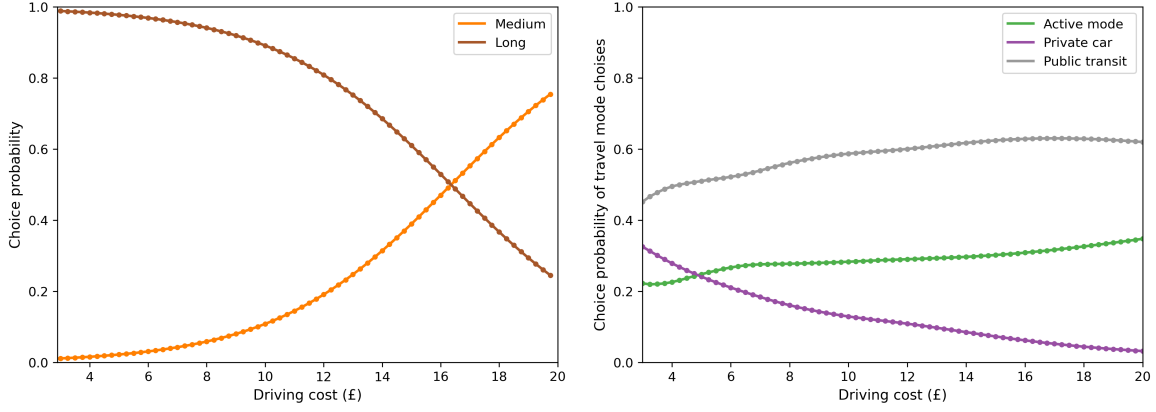


Figure 9: Substitution patterns of travel distance and travel mode choice with varying travel driving cost

### 5.3 Results of the Simulated Dataset

To clarify the differences between our approach with the typical approach widely used in behavioural modelling, we make use of a simulated dataset. Figure 10 shows the behaviour-generating process in the simulated dataset assumed by ourselves. In this graph, both collider: {traffic density perception} and non-collider: {age, gender} sets are assumed so as to clarify the role of these variables in the parameter estimation of policy (stress level) on the outcome (wait time).

The generated synthetic dataset with 2,500 pseudo-observed individuals consists of five variables, including exogenous and endogenous variables. The exogenous variables are assumed to follow the same distributions as the observational pedestrian crossing dataset and the endogenous variables (stress level, waiting time, and density perception) are generated based on the ordered logit model assumptions with a set of known parameters. Note that the generated discrete density variable serves as a proxy for density perception in our simulated dataset. Table 7 enumerates the detailed information of variables and their coefficients in our assumptions.

Table 7: Variables of synthetic dataset

Variables	Distribution	Categories	Value/Distribution of coefficient		
			Stress level	Wait time	Density perception
Gender	Binary	Yes, No	0.500	0.603	-
Age	Categorical	Age 25-29	0.950	-0.795	-
		Age 30-39	0.561	-1.410	-
		Age 40-49	2.911	-1.854	-
		Age over 50	1.975	-2.854	-
Number of cars	Categorical	One car	-0.300	-	-
		Over one car	-0.132	-	-
Density perception	Binary	Yes, No	0.500	-0.800	-

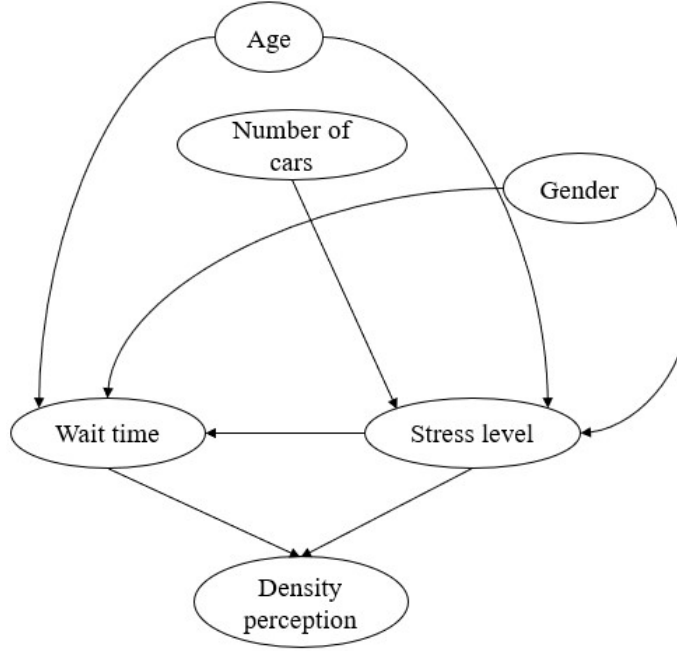


Figure 10: Causal structure of simulated dataset

As mentioned, in the literature, it is common to evaluate the impact of all logical explanatory variables on the outcome, guided by prior knowledge. However, it is of vital importance to consider that conditioning on certain variables can inadvertently create non-causal paths between variables of interest. In fact, although conditioning on explanatory variables allows us to block non-causal paths that may exist between policy variables and outcomes, the selection of conditioning variables to avoid introducing spurious associations, based on the blocking set mentioned in Section 2.2.1, is crucial for causal analysis. In the simulated dataset, density perception acts as a collider variable in such a way that conditioning on that can create bias in the estimation of causal effects between stress level and wait time. In this section, we try to recover the effect of stress level on wait time using two distinct approaches: 1) modelling the association using the aforementioned typical variable selection method commonly found in the literature, and 2) modelling the causal mechanism based on the causal data generating process. In both approaches, we utilize ResNet-based frameworks, albeit with different model specifications. In the first approach, all reasonable variables are included in Ordinal-Reslogit. Conversely, in the second approach, the models are specified based on the causal graph. The mean value of the estimated parameter for both approaches is provided in Table 8.

Comparing the result of the two approaches with the true effect demonstrates that the typical approach in which we include the density perception (collider variable) into utility function, leads to a much higher error in estimation, approximately 42.9%. However, the *CAROLINA* which is built upon the causal structure and does not consider the effect of the collider, achieves more accurate and unbiased results.

Table 8: Comparison between causal and non-causal-based models

Cause	Effect	True causal effect	Ordinal-ResLogit	<i>CAROLINA</i>
Stress level	Wait time	0.600	0.153	0.410

## 5.4 Counterfactual Analysis

In this section, we apply the generative counterfactual model structure in *CAROLINA* to generate the counterfactual data for pedestrian and London mode choice datasets. This model structure is able to address the fundamental challenge in causal inference and allows us to predict the counterfactual outcomes for each observation. We examine the impact of interventions on pedestrian wait time and mode share in the counterfactual condition. Specifically, we investigate two interventions: 1) exploring how an individual’s decisions would have changed if the stress levels were reduced to a low level for all individuals in the sample by making the walking infrastructure safer, and 2) assessing how individuals’ preferences would have been influenced if recreational amenities, like shopping malls and restaurants, were available within a 7.8 kilometres ( $\approx 5$  miles) radius from their origin, representing medium distance trips. Based on our methodology, in both datasets, we first learn the distribution of the latent variables ( $\varepsilon_i$ ) associated with the causal mechanisms of the aforementioned intervention distribution. The utilization of normalizing flow in our proposed model allows us to transition from a simple normal distribution assumption to a more representative distribution that captures the characteristics of various latent behaviours in the dataset (Kim & Mokhtarian, 2023). Figure 11 displays the visual representation of the distribution of the latent variable, which is captured by using the normalizing flow layers. The multimodal distributions illustrate that our datasets consist of multiple unobserved behaviours. Indeed, there are multiple sub-population having different unobserved behaviour constructs. In fact, by capturing a more representative latent construct, obtained through the normalizing flows technique, we can better incorporate the diverse underlying unobserved processes that contribute to the observed data into our counterfactual model. Furthermore, a comparison of the latent variable distribution between private car and public transit reveals the differences. This suggests that the latent variable likely encompasses the influence of mode-related attributes.

Secondly, the relevant structural causal mechanisms are changed based on the desired manipulation. This step is identical to intervention in the generating process in such a way that stress level is set to a low level and travel distance is reduced to medium for all individuals in the population sample of pedestrian crossing and travel behaviour dataset respectively. Eventually, we utilize deep learning-based model structures to predict the counterfactual outcome for each individual in the manipulated system. Figure 12 visualizes the impact of these interventions on the validation dataset of both behaviour systems.

Figure 12 illustrates that intervening in pedestrian stress levels totally leads to a 35.35% increase in the number of individuals who experience shorter waiting times on the sidewalk. To gain deeper insights into the specific shifts, resulting from the

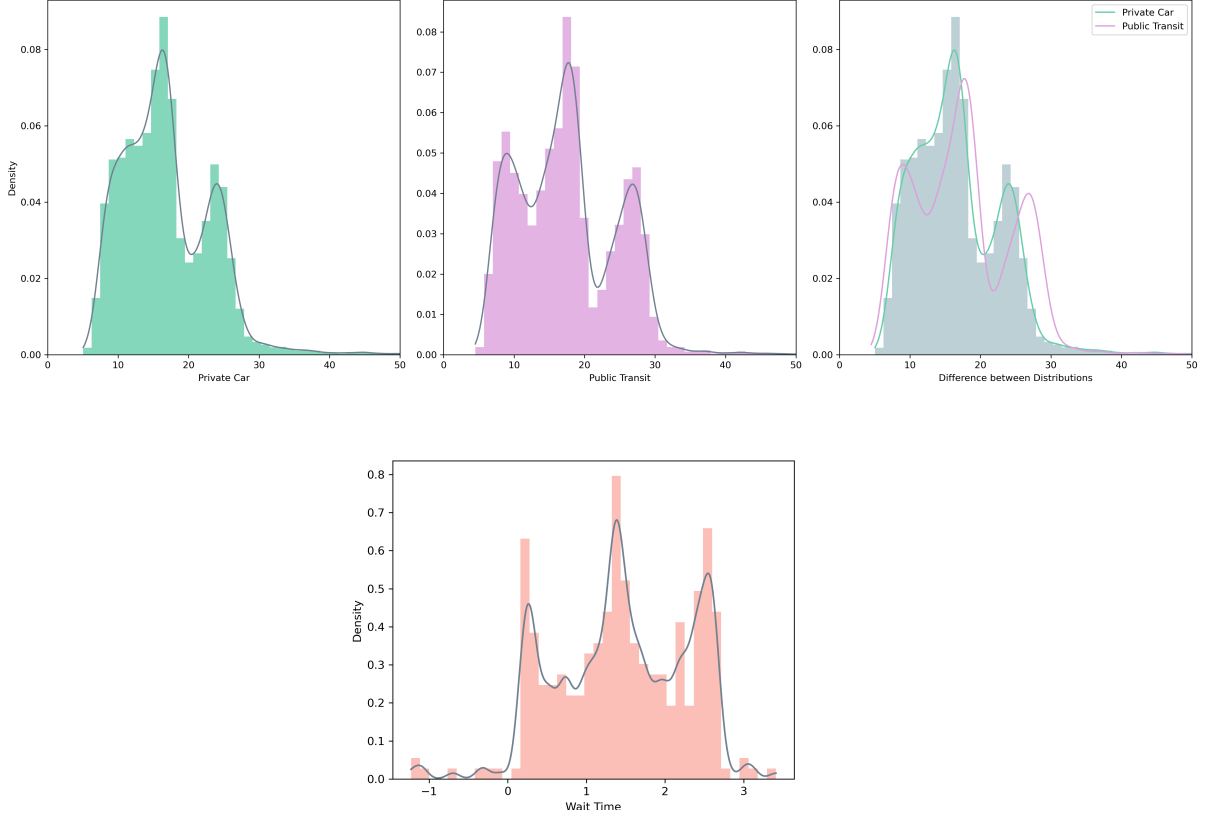


Figure 11: Distribution of the latent variable

interventions, Figure 13 presents a matrix that depicts the low-high categories comparison between the factual and counterfactual worlds. This matrix provides detailed information on how the interventions impact the distribution of waiting times among individuals. The values in the matrix represent the counts of individuals who experience longer waiting times (from low to high), shorter waiting times (from low to high), and those who experience the same waiting time as in the factual world (diagonal value) in the counterfactual condition.

Concerning travel distance, as shown in Figure 12 decreasing the travel distance to the medium category in the validation dataset, approximately increases the share of active modes such as biking and walking by 47.29%. Notably, based on the mode share matrix distribution (Figure 13), 34.65% of these individuals transition from using private cars to active modes. Conversely, a total of 6.92% individuals in the dataset, in the counterfactual world would have opted for private car usage, whereas in the factual world, they choose alternative travel modes.

## 6 Limitation

While our proposed model demonstrates significant performance, it is crucial to underscore its inherent limitations within the context of behavioural analysis. Firstly, in the case of certain completely unseen behaviours, the *CAROLINA* framework may not operate accurately. The model is constructed based on causal structure learning from the observational dataset using causal discovery algorithms. Therefore, in unfore-

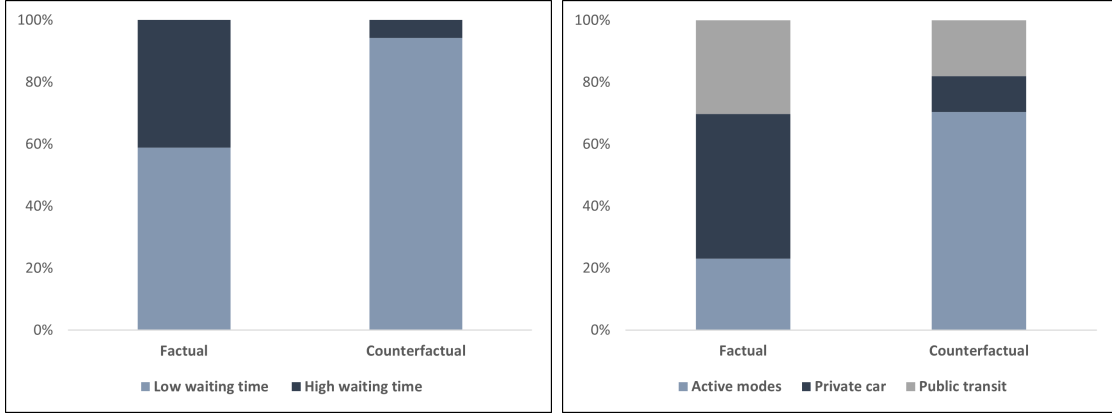


Figure 12: Impact of interventions on pedestrian wait time and travel mode shares

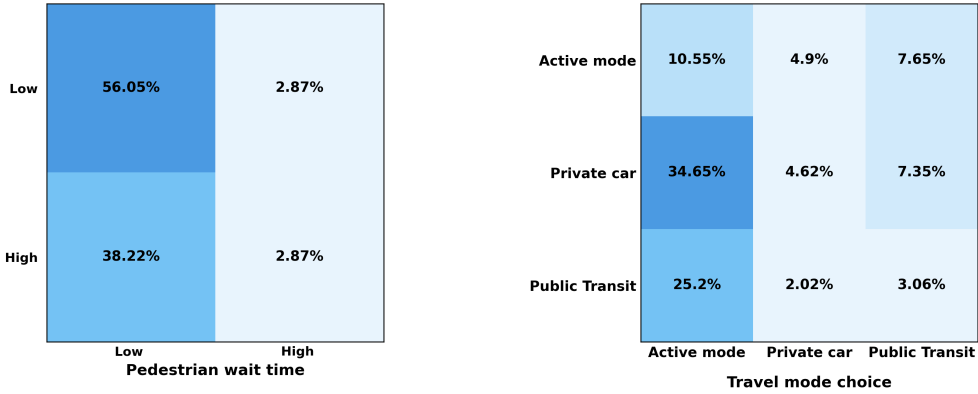


Figure 13: Categories distribution between factual and counterfactual world

seen circumstances, such as the mobility behaviour during the COVID-19 pandemic, our model would suffer from a lack of reliable causal structure, labelling this causal behavioural analysis as unpredictable. Secondly, the setting of hyperparameters considerably influences the performance of such models and the systematic identification of hyperparameters is important. Furthermore, for efficient computation of the Jacobian determinant, we employ a simple flow model that necessitates a longer sequence of transformations to provide a more flexible posterior distribution. This choice, however, renders the model computationally expensive. In addition, the training time of *CAROLINA* framework is higher than SCM-Logit in which no deep layers are applied. For example, in the London travel dataset, the training time of our proposed model is approximately six times longer than SCM-logit. By using Graphic Processing Units (GPUs) and data reduction techniques, the computational time can be decreased, but this is out of the scope of the current work.

## 7 Conclusion

This study bridges the key gaps between behavioural modelling, deep learning, and causal inference in the realm of transportation. We propose the *deep CAusal infeR-*



ence *mOdelling for traveL behavIour aNalysis* (*CAROLINA*) framework. To predict human behaviour in the counterfactual world, we propose a novel Generative Counterfactual Model within *CAROLINA* framework. The formulation of the framework utilizes ResLogit and Ordinal-ResLogit as the building blocks, which are two completely interpretable deep learning-based discrete choice models used for categorical and ordinal problems respectively. Therefore, *CAROLINA* serves as a logical extension of these existing models, while being explicitly designed for causality analysis.

*CAROLINA* enables us to identify the determining factors and confounding variables associated with the studied interventions. In addition, it can simultaneously capture unobserved heterogeneity and infer causal relationships. The use of ResLogit and Ordinal-ResLogit model structures ensures the complete interpretability of our models. As a result, our proposed approach effectively addresses the challenges of interpretability and causality that have been lacking in the application of deep learning algorithms to travel behavioural analysis. It is worth mentioning that our proposed model is still a probabilistic model structure that tries to discover the most probable causation with a certain degree of confidence.

Broadly, the counterfactual model structure facilitates the policy assessment process in a more realistic fashion. This model structure assists us in making causal inferences regarding how the individual’s choices would have been changed if transportation planners had intervened in specific aspects of the system. Our main purpose is to model interventional distribution in such a way that studied causal mechanisms are changed while other mechanisms of causal structures and the exogenous latent variables remain unchanged. In this study, we incorporate the Normalizing Flow technique into the Variational AutoEncoder framework (VAE) so as to infer the latent variable distribution, representing all individual classes in a dataset. This component of the counterfactual model structure is specifically called Flow-based Variational Autoencoder (FVAE) in the framework.

To assess the performance of our proposed models, we utilize two distinct datasets: 1) pedestrian crossing behaviour in the presence of Automated Vehicles (AVs), collected through a virtual reality simulation, and 2) a revealed Preference (RP) London travel demand dataset. Based on the obtained causal structures, our analysis in the first dataset primarily centers around the causal relationship between stress levels and pedestrian wait times. Concerning the second dataset, we also analyze the causal process in which individuals choose medium or long travel distances and examine how these choices directly influence their overall travel behaviour. The results show that the *CAROLINA* framework outperforms the conventional structural causal model (SCM) built on Multinomial Logit (MNL) and Ordered Logit Models. More importantly, we examine the performance of our causal structure-based model with the association-based approach employed in travel behavioural modelling by using a simulated dataset. The result of this evaluation highlights the critical importance of adjusting for confounding variables.

In terms of the counterfactual world of datasets, we examine the impact of interventions on pedestrian wait time and mode share in pedestrian crossing behaviour and travel behaviour datasets respectively. The results reveal a significant impact of intervening in pedestrian stress levels, resulting in a substantial 35.35% increase in the number of individuals experiencing shorter waiting times on the sidewalk. Regarding the second dataset, we observed that by reducing the travel distance to the medium

category, there is an approximate 47.29% increase in the proportion of active modes, including biking and walking.

Our study tries to initiate a new research area building upon the critique developed by Brathwaite and Walker, 2018. In light of the findings presented in this study, several future research and potential improvements emerge. Firstly, the analysis of unobserved confounders in the factual world and their edges towards other observed variables can be one future direction. Furthermore, further researchers in the field of causality analysis can make a comparison between the performance of our proposed models and other approaches. In order to evaluate and determine the feasibility of the idea of the generative counterfactual model, we can focus on Backcasting method in future studies, involving working backward from the future to the present by using a real temporal dataset. This approach provides valuable insights into the effectiveness of the counterfactual model structure. This evaluation helps us improve the model performance by revising the algorithms or model parameters. For example, in our counterfactual model, we utilize normalizing flow to estimate the distribution of exogenous latent variables. Yet, there may be potential for enhancing this aspect of our model by exploring other flow transformations or alternative algorithms. In addition, future studies can mainly focus on causal structure learning by applying different causal discovery algorithms. Regarding the deep learning aspect of our model, it is worth noting that regularization techniques were not employed in this study to ensure a fair comparison between our proposed model and econometric models. However, future studies could enhance our frameworks by focusing on regularization techniques and tuning hyperparameters. It is worth mentioning that particularly in terms of pedestrian crossing behaviour in the presence of Automated Vehicles (AVs), we require more causal-based research on different datasets for inferring true causal structures.

## Acknowledgements

This research was funded by a grant from the Canada Research Chair program in Disruptive Transportation Technologies and Services (CRC-2021-00480) and NSERC Discovery (RGPIN-2020-04492) fund.

## Appendices

### A Pseudocodes

The pseudocodes for the algorithms in *CAROLINA* framework are outlined here.

---

**Algorithm 1** Algorithm of deep structural causal model in *CAROLINA*

---

**Require:**  $G = (X, \xi)$  where  $X$  is the set of variables and  $\xi$  is the set of dependencies

**Ensure:**  $Pa(x_i) = \emptyset$ ,  $seq = x_{outcome}$ ,  $x_{ex} = \emptyset$ ,  $x_{des} = \emptyset$ ,  $x_{en} = \emptyset$

```
for  $i = 1$  to  $n$  do
  for  $j = 1$  to  $n$ , where  $j \neq i$  do
    if  $I(\xi_{ji}) \neq 0$  then
       $Pa(x_i) \leftarrow x_j$ 
    else if  $Pa(x_i) = Pa(x_i)$  then
      end if
    end for
  end for
  if  $Pa(x_i) = \emptyset$  then
     $x_{ex} \leftarrow x_i$ 
  end if
  if  $Pa(x_i) \neq \emptyset$  then
    for  $j = 1$  to  $n$ , where  $j \neq i$  do
      if  $I(\xi_{ij}) = 0$  then
         $x_{des} \leftarrow x_i$ 
      else if  $x_{en} \leftarrow x_i$  then
        end if
      end for
    end if
    for  $x_i$  in  $seq$  do
      if visited[ $x_i$ ] = False then
        for  $x_j$  in  $Pa(x_i)$  do
          if  $x_j \in x_{en}$  then
             $seq[\text{len}(seq) + 1] \leftarrow x_j$ 
          else if  $seq = seq$  then
            end if
          end for
          visited[ $x_i$ ] = True
        else if : then Break
        end if
      end for
    for  $x_i = seq[\text{len}(seq)]$  to  $seq[0]$  do
      Train ResNet-based model structures
      if  $x_i$ : categorical then
        Calculate:  $P(x_i = k | Pa_k^i) = \frac{\exp(\beta_k Pa_k^i + g_k^i)}{\exp\left(\sum_{k=1}^K \beta_k Pa_k^i + g_k^i\right)}$ 
      else if  $x_i$ : ordinal then
        Calculate:  $P(x_i = k | Pa_k^i) = \sigma\left(\left(\sum_{k=1}^K W_k(\beta_k Pa_k^i + g_k^i)\right) + b_k\right)$ 
      end if
    end for
  end for
  Calculate:  $\prod_{i=1}^I P\left(x_i | Pa_i\right)$ 
```

---

---

**Algorithm 2** Algorithm of counterfactual model structure in *CAROLINA*

---

**Require:**  $G = (x, \xi)$ ,  $Pa(x_i)$ ,  $f_i(Pa_i, \beta_i)$  and  $seq$

**for** each  $x_i \in (seq)$  **do**

1. Abduction:

Initialize Encoder parameters  $\theta_{\text{enc}}$ , Decoder parameters  $\theta_{\text{dec}}$ , Normalizing flow parameters  $\theta_{\text{flow}}$  randomly.

**for** each epoch **do**

**for** each mini-batch  $B$  **do**

Reset gradients.

**for** each sample  $x_n$  in  $B$  **do**

Encode  $x_n$  to obtain mean and log-variance parameters  $\mu, \sigma^2$  using  $\theta_{\text{enc}}$ .

Sample  $\gamma_0 \sim \mathcal{N}(\mu, \sigma^2)$ .

Apply  $K$  normalizing flows to  $\gamma_0$  to obtain transformed latent variable  $\gamma_k$  and log determinant of Jacobian  $J$ .

Reconstruct  $x'_n$  using  $\gamma_k$  and  $\theta_{\text{dec}}$ .

Compute reconstruction loss ( $L_{\text{recon}}$ ) between  $x_n$  and  $x'_n$ .

Compute KL divergence loss ( $L_{\text{KL}}$ ) between the approximate latent distribution and true distribution.

Compute total loss  $L_{\text{total}} = L_{\text{recon}} + L_{\text{KL}}$ .

Accumulate gradients of  $L_{\text{total}}$  w.r.t.  $\theta_{\text{enc}}$ ,  $\theta_{\text{dec}}$ , and  $\theta_{\text{flow}}$ .

**end for**

Update parameters using the optimizer.

**end for**

**end for**

2. Manipulation:

Interventional CAROLINA: Manipulate the causal graph and accordingly CAROLINA either in the soft or hard operation

3. Prediction:

Sample  $\gamma_i \sim q_k$

Compute latent component of causal structures:  $\varepsilon_i = \gamma_i - f_i(Pa_i, \beta_i)$

Predict  $x_{\text{counterfactual}}$  for  $x_{\text{outcome}}$  using the Interventional CAROLINA.

**end for**

---

## B Counterfactual Modelling: Definitions

Three levels of counterfactual modelling are defined as follows (Figure ??):

- **Abduction:** It refers to the process of identifying the causal relationships and their mechanisms underlying the observed data. Furthermore, another aim of the abduction level is to infer the probability distribution of  $P(\varepsilon_i|x_i)$ , which represents the likelihood of different values of the exogenous latent variables in the real world. By estimating the latent constructs, we gain insight into the values that are a partial part of generating the endogenous variables. This step helps us to understand the uncertainty and variability in the system that is assumed to be identical to the counterfactual world.
- **Manipulation:** This level involves specifying the intervention(s) or hypothetical policy and manipulating the system either in the soft or hard way, resulting in an interventional SCM corresponding to intervention/counterfactual distribution.
- **Prediction:** The prediction level focuses on estimating the counterfactual outcome that would have occurred under the intervention of interest.

Figure 14 also compares these steps with the steps involved in the association based prediction approach.

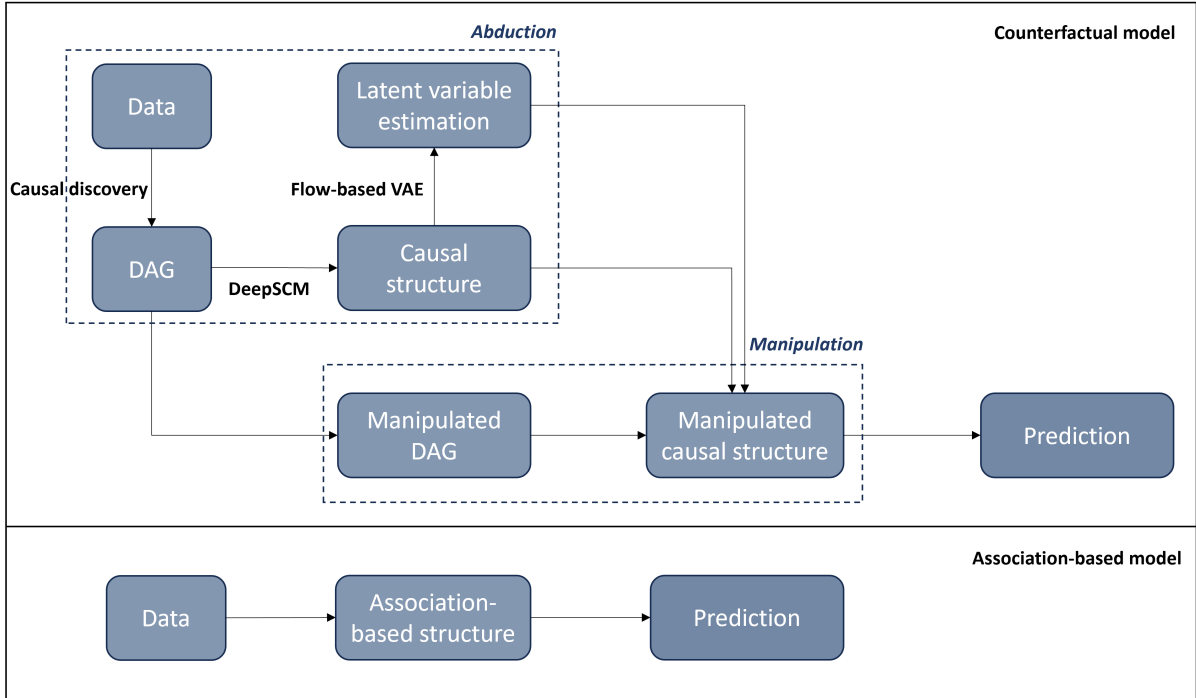


Figure 14: Three levels of counterfactual model and comparison with conventional prediction approach

## References

- Bergstra, J., & Bengio, Y. (2012). Random search for hyper-parameter optimization. *Journal of machine learning research*, 13(2).
- Brathwaite, T., & Walker, J. L. (2018). Causal inference in travel demand modeling (and the lack thereof). *Journal of choice modelling*, 26, 1–18.
- Cao, X., & Fan, Y. (2012). Exploring the influences of density on travel behavior using propensity score matching. *Environment and Planning B: Planning and Design*, 39(3), 459–470.
- Cao, X., Xu, Z., & Fan, Y. (2010). Exploring the connections among residential location, self-selection, and driving: Propensity score matching with multiple treatments. *Transportation research part A: policy and practice*, 44(10), 797–805.
- Chickering, D. M. (2002). Optimal structure identification with greedy search. *Journal of machine learning research*, 3(Nov), 507–554.
- Farooq, B., Cherchi, E., & Sobhani, A. (2018). Virtual immersive reality for stated preference travel behavior experiments: A case study of autonomous vehicles on urban roads. *Transportation research record*, 2672(50), 35–45.
- Golob, T. F. (2003). Structural equation modeling for travel behavior research. *Transportation Research Part B: Methodological*, 37(1), 1–25.
- Goodfellow, I., Bengio, Y., & Courville, A. (2016). *Deep learning*. MIT press.
- Goudet, O., Kalainathan, D., Caillou, P., Guyon, I., Lopez-Paz, D., & Sebag, M. (2018). Learning functional causal models with generative neural networks. *Explainable and interpretable models in computer vision and machine learning*, 39–80.
- Hillel, T., Bierlaire, M., Elshafie, M. Z., & Jin, Y. (2021). A systematic review of machine learning classification methodologies for modelling passenger mode choice. *Journal of choice modelling*, 38, 100221.
- Hillel, T., Elshafie, M. Z., & Jin, Y. (2018). Recreating passenger mode choice-sets for transport simulation: A case study of london, uk. *Proceedings of the Institution of Civil Engineers-Smart Infrastructure and Construction*, 171(1), 29–42.
- Hoyer, P., Janzing, D., Mooij, J. M., Peters, J., & Schölkopf, B. (2008). Nonlinear causal discovery with additive noise models. *Advances in neural information processing systems*, 21.
- Jiang, B. (2013). Head/tail breaks: A new classification scheme for data with a heavy-tailed distribution. *The Professional Geographer*, 65(3), 482–494.
- Kalatian, A., & Farooq, B. (2021). Decoding pedestrian and automated vehicle interactions using immersive virtual reality and interpretable deep learning. *Transportation research part C: emerging technologies*, 124, 102962.
- Kamal, K., & Farooq, B. (2022). Debaised machine learning for estimating the causal effect of urban traffic on pedestrian crossing behavior. *Transportation Research Record*, 03611981231152246.
- Kamal, K., & Farooq, B. (2024). Ordinal-reslogit: Interpretable deep residual neural networks for ordered choices. *Journal of Choice Modelling*, 50, 100454.
- Karlaftis, M. G., & Vlahogianni, E. I. (2011). Statistical methods versus neural networks in transportation research: Differences, similarities and some insights. *Transportation Research Part C: Emerging Technologies*, 19(3), 387–399.

- Kim, S. H., & Mokhtarian, P. L. (2023). Finite mixture (or latent class) modeling in transportation: Trends, usage, potential, and future directions. *Transportation Research Part B: Methodological*, 172, 134–173.
- Kingma, D. P., Salimans, T., Jozefowicz, R., Chen, X., Sutskever, I., & Welling, M. (2016). Improved variational inference with inverse autoregressive flow. *Advances in neural information processing systems*, 29.
- Kingma, D. P., & Welling, M. (2019). An introduction to variational autoencoders. *Foundations and Trends® in Machine Learning*, 12(4), 307–392.
- Kobyzev, I., Prince, S. J., & Brubaker, M. A. (2020). Normalizing flows: An introduction and review of current methods. *IEEE transactions on pattern analysis and machine intelligence*, 43(11), 3964–3979.
- Mokhtarian, P. L., & Cao, X. (2008). Examining the impacts of residential self-selection on travel behavior: A focus on methodologies. *Transportation Research Part B: Methodological*, 42(3), 204–228.
- Mokhtarian, P. L., & van Herick, D. (2016). Quantifying residential self-selection effects: A review of methods and findings from applications of propensity score and sample selection approaches. *Journal of Transport and Land Use*, 9(1), 9–28.
- Mudassar, M., Kalatian, A., & Farooq, B. (2022). Analysis of pedestrian stress level using gsr sensor in virtual immersive reality. *Collective Dynamics*, 6.
- Nogueira, A. R., Pugnana, A., Ruggieri, S., Pedreschi, D., & Gama, J. (2022). Methods and tools for causal discovery and causal inference. *Wiley interdisciplinary reviews: data mining and knowledge discovery*, 12(2), e1449.
- Papamakarios, G., Nalisnick, E., Rezende, D. J., Mohamed, S., & Lakshminarayanan, B. (2021). Normalizing flows for probabilistic modeling and inference. *The Journal of Machine Learning Research*, 22(1), 2617–2680.
- Parsa, A. B., Kamal, K., Taghipour, H., & Mohammadian, A. K. (2019). *Does security of neighborhoods affect non-mandatory trips? a copula-based joint multinomial-ordinal model of mode and trip distance choices* (tech. rep.).
- Pearl, J. (2009a). Causal inference in statistics: An overview. *Statistics surveys*, 3, 96–146.
- Pearl, J. (2009b). *Causality*. Cambridge university press.
- Peters, J., Janzing, D., & Schölkopf, B. (2017). *Elements of causal inference: Foundations and learning algorithms*. The MIT Press.
- Ramsey, J., Glymour, M., Sanchez-Romero, R., & Glymour, C. (2017). A million variables and more: The fast greedy equivalence search algorithm for learning high-dimensional graphical causal models, with an application to functional magnetic resonance images. *International journal of data science and analytics*, 3, 121–129.
- Rezende, D., & Mohamed, S. (2015). Variational inference with normalizing flows. *International conference on machine learning*, 1530–1538.
- Rubin, D. B. (2019). Essential concepts of causal inference: A remarkable history and an intriguing future. *Biostatistics & Epidemiology*, 3(1), 140–155.
- Shen, X., Ma, S., Vemuri, P., & Simon, G. (2020). Challenges and opportunities with causal discovery algorithms: Application to alzheimer’s pathophysiology. *Scientific reports*, 10(1), 1–12.



- Shimizu, S., Hoyer, P. O., Hyvärinen, A., Kerminen, A., & Jordan, M. (2006). A linear non-gaussian acyclic model for causal discovery. *Journal of Machine Learning Research*, 7(10).
- Shpitser, I., & Pearl, J. (2006). Identification of joint interventional distributions in recursive semi-markovian causal models. *Proceedings of the National Conference on Artificial Intelligence*, 21(2), 1219.
- Siffringer, B., Lurkin, V., & Alahi, A. (2020). Enhancing discrete choice models with representation learning. *Transportation Research Part B: Methodological*, 140, 236–261.
- Spirtes, P. (2010). Introduction to causal inference. *Journal of Machine Learning Research*, 11(5).
- Spirtes, P., Glymour, C. N., & Scheines, R. (2000). *Causation, prediction, and search*. MIT press.
- Spissu, E., Pinjari, A. R., Pendyala, R. M., & Bhat, C. R. (2009). A copula-based joint multinomial discrete–continuous model of vehicle type choice and miles of travel. *Transportation*, 36, 403–422.
- Vance, C., & Hedel, R. (2007). The impact of urban form on automobile travel: Disentangling causation from correlation. *Transportation*, 34, 575–588.
- Wang & Ross, C. L. (2018). Machine learning travel mode choices: Comparing the performance of an extreme gradient boosting model with a multinomial logit model. *Transportation Research Record*, 2672(47), 35–45.
- Wang, S., Mo, B., & Zhao, J. (2020). Deep neural networks for choice analysis: Architecture design with alternative-specific utility functions. *Transportation Research Part C: Emerging Technologies*, 112, 234–251.
- Wong, M., & Farooq, B. (2021). Reslogit: A residual neural network logit model for data-driven choice modelling. *Transportation Research Part C: Emerging Technologies*, 126, 103050.
- Yao, L., Chu, Z., Li, S., Li, Y., Gao, J., & Zhang, A. (2021). A survey on causal inference. *ACM Transactions on Knowledge Discovery from Data (TKDD)*, 15(5), 1–46.